Emergent Materials
https://doi.org/10.1007/s42247-024-00760-8

REVIEW ARTICLE

Research progress on flexible WO_3 based thin film electrodes for supercapacitor applications: a comprehensive review

Elif Muslu[1] · Esin Eren[1] · Aysegul Uygun Oksuz[1]

Received: 21 December 2023 / Accepted: 29 May 2024
© The Author(s) 2024

Abstract
In recent years, there has been significant research interest in flexible supercapacitors as energy storage devices for enhancing wearable and portable electronics. This is due to their lightweight nature, high power density, excellent cyclic durability, fast charge/discharge rate, and robust mechanical integrity. Flexible supercapacitors offer the potential to revolutionize the field of energy storage by providing efficient and reliable power sources for various portable and wearable applications. Thin film based electrodes, as one of the ingredients of flexible supercapacitors, have a considerable role on the electrochemical performance of flexible supercapacitors. Tungsten oxide (WO_3), a transition metal oxide (TMO), is a highly desirable electrode material for flexible supercapacitor applications. It offers several advantages, including low cost, environmental friendliness, inherent conductivity, versatile oxidation states, and high theoretical capacity. These properties make WO_3 an excellent choice for developing efficient and sustainable energy storage solutions. Specially, this review provides current developments on the WO_3 based thin film electrodes toward flexible supercapacitors. We will present the focus attention on the charge storage mechanisms, fabrication strategies, and characterization methods employed in this field.

Keywords Flexible · Tungsten oxide · Thin film · Supercapacitor

1 Introduction

In today's energy landscape, there is a growing need for alternative energy sources due to the reliance on fossil fuels, their limited availability, and concerns about resource sustainability [1]. Electrochemical energy storage has emerged as a promising solution, with advancements in supercapacitors (SCs), lithium-ion batteries (LIBs), and alkaline batteries. While LIBs offer high energy densities, they face limitations with respect to cycle life and power density [1]. Supercapacitors, on the other hand, have gained attention as next-generation power devices due to their higher power density compared to batteries and higher energy density compared to traditional capacitors [2, 3].

Supercapacitors can be classified into electric double-layer capacitors and pseudocapacitors based on their charge storage mechanism [4]. The choice of electrode material plays a critical role in determining the electrochemical performance. Nanostructured semiconductor metal oxides have shown promise in enhancing the performance of supercapacitor electrodes [5–7]. Additionally, metal oxide materials have been explored for flexible supercapacitor applications, which require small volume, light weight, elevated safety, and good mechanical durability [8]. Flexible energy storage having small volume, light weight, elevated safety, good mechanical durability, perfect electrochemical performance displays great demand. Flexible supercapacitors are displayed to be encouraging candidates because of their powerful mechanical flexibility, excellent safety and almost unchangeable performance even under mechanical deformations of diverse degrees. However, they are necessary for excellent electrical conductivity, high energy density and long cycle life to improve their practical flexible application [9].

Among the pseudocapacitive materials, transition metal oxides (TMOs) have been extensively studied [10]. WO_3, in particular, has garnered interest due to its excellent electron transport properties and corrosion resistance [11–13]. Furthermore, WO_3 is an attractive electrode material due to superior capacitance performance compared to the other

✉ Elif Muslu
elifmuslu@sdu.edu.tr

✉ Aysegul Uygun Oksuz
ayseguluygun@sdu.edu.tr

[1] Department of Chemistry, Faculty of Engineering and Natural Sciences, Suleyman Demirel University, 32260 Isparta, Turkey

Published online: 25 June 2024

metal oxide materials (Fig. 1) [14–17]. This advantage is derived from its cost-effectiveness, straightforward synthesis process, outstanding conductivity, and a high theoretical capacitance of 1112 F/g [15]. Numerous scientists have made significant efforts to investigate WO_3 as a pseudocapacitive electrode material WO_3 stands out as a popular choice for anode material in material science. Its appeal lies in its wide band gap, making it an effective n-type semiconductor. Additionally, WO_3 possesses inherent properties such as high packing density exceeding 7 g/cm^3 and exhibits diverse oxidation states ranging from +2 to +6. Its oxygen deficiency further enhances its suitability for pseudocapacitive storage applications [18].

WO_3 exists in multiple polymorphs, characterized by a variety of crystal structures. These structures primarily arise from the arrangement of WO_6 octahedra, which connect through their corners and edges. WO_3 demonstrates a diversity of crystal forms, including monoclinic, triclinic, orthorhombic, tetragonal, cubic, and hexagonal (Table 1) [27].

These variations are the result of the tilt and rotation of WO_6 octahedra, as well as the displacement of W cations. The structural configuration of WO_3 allows for numerous interstitial sites, which are advantageous for ion sorption and insertion. This feature makes the hexagonal form of WO_3 particularly valuable in energy storage applications, serving as an effective host for intercalation. Moreover, WO_3 exhibits sub-stoichiometric phases, known as Magneli phases, with formulas represented as W_nO_{3n-1} and W_nO_{3n-2}. These phases contribute to enhanced electrical conductivity through the presence of oxygen vacancies. Specifically, the hexagonal phase of WO_3 is found to be exceptionally suited for use in pseudocapacitors, thanks to its large tunnels that facilitate easy ion insertion [28].

Regarding amorphous WO_3, its substantial capacity for small ions contributes positively to high optical modulation. Additionally, the presence of multiple types of transport channels and defects associated with oxygen vacancies enhances ion diffusion, facilitating rapid colour switching. However, its metastable microstructure and limited chemical stability can slow down its cyclic operation. In contrast, crystalline WO_3 exhibits higher conductivity, and its stable microstructure ensures enhanced chemical and structural stability. Nevertheless, its singular transport tunnel and dense structure result in relatively low ion diffusion rates [29].

Table 1 Representations of crystal structures of WO_3

Crystal structure	Symmetry
δ-WO_3	Triclinic
γ-WO_3	Monoclinic
β-WO_3	Orthorhombic
α-WO_3	Tetragonal
Cubic WO_3	Cubic
h-WO_3	Hexagonal

In recent advancements in WO_3-based flexible supercapacitor applications, several approaches have been promised to use the WO_3 alone or WO_3 with high mass loading or composites with different materials as electrode materials [18] and numerous researchers have attempted to merge the benefits of both amorphous and crystalline structures at the nanoscale, as well [29].

WO_3 is recognized for its stability and rigidity. However, its fabrication in thin film and nanostructured forms, such as nanosheets, reveals enhanced functional properties. These nanoarchitectures offer a high surface area and preferentially exposed facets, significantly improving reaction kinetics vital for electrochromic devices and charge storage applications—areas where bulk forms are less effective. Despite W element's higher cost, the remarkable performance improvements and the efficiency of nanostructured films justify the synthesis of WO_3 in these forms.

Transitioning from bulk to thin film WO_3 does not necessarily lead to a proportional cost increase. Advances in synthesis techniques, including nano structuring and the creation

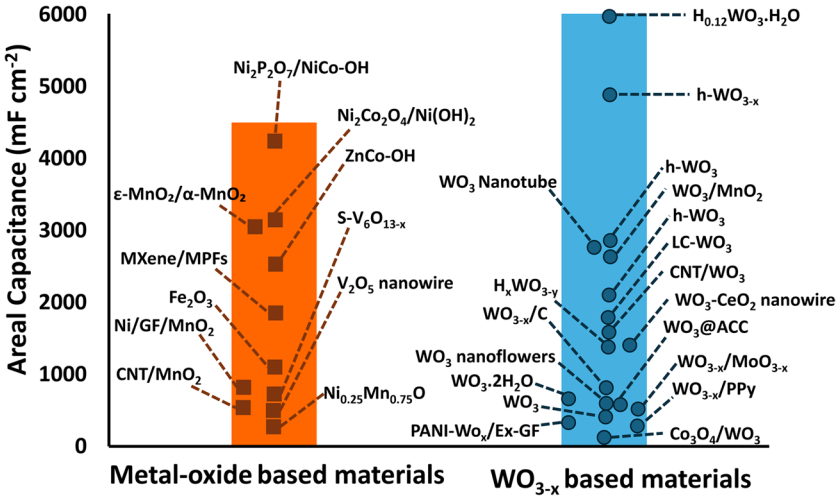


Fig. 1 Specific capacitances of WO_3-based electrode materials compared with metal oxide-based materials. Adapted from [19] and updated with [20–26]

جامعة قطر QATAR UNIVERSITY

of hybrid films, have aimed to boost WO_3's performance. These methods ensure efficient material use, potentially offsetting the cost implications of employing tungsten. Furthermore, thin film technology intrinsically requires less material than bulk forms, aiding cost efficiency. The detailed preparation methods and performance enhancement strategies underscore technological progress, maintaining cost-effectiveness while significantly enhancing functionality [27].

As the shift towards wearable technology and portable electronics grows, the demand for energy storage solutions that are efficient, versatile, and mechanically resilient becomes paramount. Here, flexible supercapacitors emerge as leaders, offering unmatched advantages in durability, adaptability to various form factors, and mechanical integrity [30]. WO_3's inherent flexibility is crucial for high performance under mechanical stress, essential for integrating into wearable electronics and smart textiles [31].

Distinct from other flexible electrode materials, WO_3 excels due to its multiple oxidation states, eco-friendliness, affordability, and high theoretical capacity. Its adaptability to various thin-film fabrication strategies markedly boosts the electrochemical performance and mechanical robustness of supercapacitors. WO_3 -based electrodes provide a balanced mix of high energy storage, swift charge/discharge rates, and outstanding cyclic durability, making them ideally suited for flexible use [32].

In comparative studies and practical deployments, WO_3 -based flexible supercapacitors have shown superior energy densities and quicker charging times. WO_3's unique properties facilitate the creation of electrodes that surpass traditional materials, thanks to its efficient use of pseudocapacitive properties. The indicates a significant increase in energy storage technology for flexible applications.

While incorporating WO_3 into flexible supercapacitor designs presents challenges, recent advances in synthesis, composite formulations, and electrode architecture have made it possible to overcome these obstacles. Progress in nanotechnology and materials science has led to WO_3-based electrodes with improved conductivity, flexibility, and electrochemical stability, ensuring their effective use in flexible supercapacitors.

In this review, our focus lies on flexible thin film electrode materials based on WO_3 for supercapacitor applications. We will emphasize the charge historical timeline, storage mechanisms, fabrication strategies, and characterization methods employed in this field.

2 Outline

2.1 Historical timeline of WO_3 based thin film electrodes

In 1841, chemist Robert Oxland pioneered procedures for preparing WO_3 and sodium tungstate, securing patents and laying the foundation for systematic tungsten chemistry [33]. The early 2000s saw pivotal studies on WO_3 electrochemical properties, crucial for energy storage devices [19, 34]. Flexible thin film deposition breakthroughs enabled WO_3 thin film fabrication on flexible substrates, propelling flexible supercapacitor development [35]. Noteworthy was the 2010-2011 creation of flexible supercapacitors featuring WO_3 electrodes, showcasing their real-world potential [36, 37].

Optimization efforts focused on WO_3 films, including nanorod synthesis enhancing pseudocapacitive properties [38]. Advanced techniques, like nano structuring and surface morphology engineering, improved capacitance and kinetics [39]. The hydrothermal method produced WO_3 nanotubes based flexible nanostructure, enhancing specific capacitance and cycling performance in 2017s [20].

In 2019, Sun et al. integrated perovskite photodetectors with WO_3 based electrochromic supercapacitors, enabling real-time monitoring and potential device health management [28]. Presently, MXene, vital for supercapacitors, faces challenges due to self-restacking. Introducing surface charged modified WO_3 nanorods within MXene layers overcomes this, yielding superior performance [29].

Öztetik et al. substituted MXene -doped WO_3 layers have been successfully fabricated on indium tin oxide (ITO) coated glass substrate. Thermionic vacuum arc was chosen as the preferred coating technology for the production of doped electrodes, as it is capable of depositing high-quality thin films. As it was widely recognized, the process of doping MXene significantly enhances the current density (3.4 mA/cm^2), leading to a substantial increase in the spaces and volumes within the 2D sheets of materials. They emphasized the utilization of 2D nanomaterial WO_3 holds significant promise for conducting electrochromic and battery research [40].

Figure 2 summarizes the historical story of the WO_3 based electrodes for supercapacitors.

2.2 Principles of energy storage mechanism in supercapacitors

Supercapacitors possess two main mechanisms for energy storage: electric double-layer capacitors (EDLCs) and pseudocapacitors (PCs) (Fig. 3) [41]. EDLCs store energy by adsorbing and desorbing ions at the electrode-electrolyte interface, whereas PCs generate and store energy through surface Faradaic redox reactions. These distinct mechanisms ensure efficient energy storage in supercapacitors, presenting promising possibilities for various applications [42–44]. While EDLCs offer higher stability due to the absence of redox reactions in the electrode materials, PCs offer higher capacitance values [44, 45]. As a result, researchers have sought to develop hybrid materials that combine the stability of EDLCs with the high capacitance of PCs [46, 47].

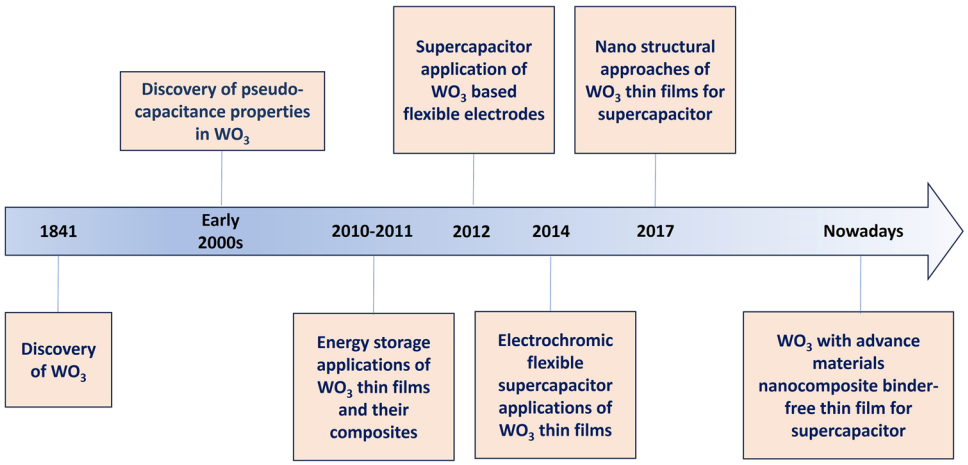


Fig. 2 Historical timeline of WO_3 based thin films for supercapacitors

The hybrid supercapacitor combines the mechanisms of both EDLCs and PCs, resulting in an energy storage and release mechanism that incorporates both non-Faradaic and Faradaic reactions [48, 49]. The energy storage and release mechanism of EDLCs is based on the nanoscale charge separation at the electrochemical interface of the electrode and electrolyte, while PCs are based on Faradaic reactions with high energy electrode materials [2, 50, 51].

Ternary compounds are a class of hybrid material known for their exceptional cyclic stability and retention when employed in supercapacitors. These consist of three constituent compounds that facilitate the rapid transfer of charge ions within the electrolyte, enabling swift redox reactions between the electrode and electrolyte [52]. Consequently, they manifest improved intermolecular interactions, enhanced surface area, expanded pore volume, and higher compaction density, making them exceptionally well-suited for integration in supercapacitor applications [47]. Furthermore, ternary-based compounds outperform single or double-component compounds, showcasing remarkable super-capacitive performance and offering a diverse range of superior both physical and chemical features [53].

In a supercapacitor, two metal electrode plates are immersed in an electrolytic solution containing cations and anions. One electrode undergoes cation accumulation through the charging process, while the other experiences anion accumulation. This leads to the formation of an electric double layer, where cations are attracted to the negatively charged electrode and anions are attracted to the positively charged electrode within the electrolyte. However, the longevity of stored charges in a supercapacitor is limited due to the impact of breakdown voltage and stray electric fields, which diminish the overall field

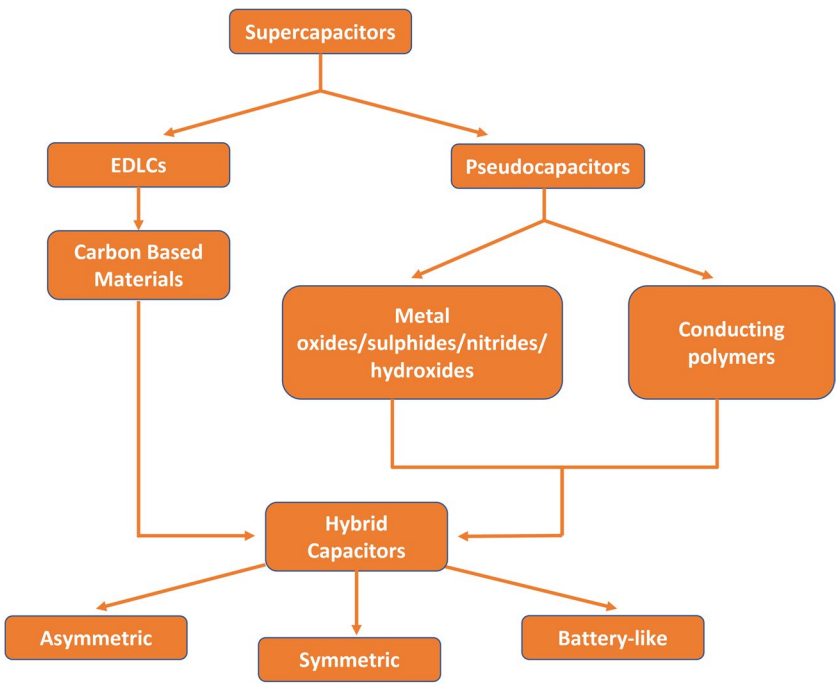


Fig. 3 Classification of supercapacitors based on their storage mechanisms

جامعة قطر QATAR UNIVERSITY

strength of the stored charges. Discharging a supercapacitor can also be influenced by various factors [1].

2.2.1 Breakdown voltage

Fast discharging of supercapacitors can be caused by various factors, among which low breakdown voltage plays a crucial role, especially under conditions of extreme current changes. At this stage, the thermal motion of atoms at room temperature, which was initially characterized by moderate random vibrations, transforms into more dynamic movements resembling the sudden onset of turbulent flow within a streamlined system. As the breakdown voltage increases, the strength of the supercapacitor diminishes at a certain point. This not only causes the loss of its electrostatic field, but also its ability to attract charges. However, once the supercapacitor is charged, it regains its electrostatic attraction and capacity to accumulate electric charges [1, 54, 55].

Generally, the breakdown voltage is the most critical factor affecting the performance of supercapacitors. In particular, electrodes based on metal oxides, such as WO_3-based electrodes, exhibit a lower breakdown voltage. This characteristic enables the utilization of smaller, more cost-effective, and safer power supplies, as it reduces the voltage required to initiate the breakdown process and facilitates the generation of electrons or ions in the discharge region [56, 57].

2.2.2 Suboptimal storage practices

SCs have clearly marked positive and negative points, and their proper storage is crucial for maintaining their capacity. Stacking them with positive points together can lead to faster capacity loss. Instead, it is recommended to arrange them in a configuration where the positive electrode of one supercapacitor is connected to the negative electrode of another, allowing for efficient charge transfer and maintaining their electrical fields through mutual attraction. Alternatively, supplementary material called a "keeper" can be placed across the electrode plates to preserve the strength and orderliness of the charges [1, 58].

2.2.3 Magnetic interaction

When electric charges are in motion, they exhibit magnetic properties and experience the Lorentz force. This force, denoted by

$$F = q\,(v \times B) = qvB\ \sin\theta \tag{1}$$

The magnitude of the force is determined by the product of the charge, q, velocity, v, magnetic field strength, B, and the sine of the angle, θ between the velocity vector and the magnetic field direction. During the charging process of a supercapacitor, the ions within the electrolyte undergo a 90° angle descent onto the electrode plate. This specific angle maximizes the force experienced by the ions, leading to an increase in power density. During the discharge process, as the supercapacitor releases stored energy, there is a variation in the angle between the v and B. This change in angle leads to a decrease in the magnitude of the Lorentz force and subsequently affects the energy density of the system. This phenomenon can be observed in Electrochemical Impedance Spectroscopy (EIS) studies, indicating the presence of induction. Additionally, Nuclear Magnetic Resonance (NMR) studies can provide supporting evidence for this theory. The explanation for this effect lies within the relativistic theory. To gain a comprehensive understanding of the internal processes occurring within a supercapacitor, a detailed analysis of each characterization tool is necessary [1, 59, 60].

While evaluating in terms of the component of the supercapacitor, WO_3 based electrode itself is not inherently magnetic, as it is primarily an insulating material with a monoclinic crystal structure. Therefore, WO_3 based electrodes in supercapacitors typically do not exhibit significant magnetic effects.

2.3 Types of supercapacitors

Supercapacitors are electronic devices that are used to store large quantities of electric charge. Unlike traditional dielectric capacitors, supercapacitors have two main mechanisms to accumulate EDLCs and PCs. The capacitance, C of a supercapacitor can be calculated using (2) [61–63]:

$$C = Q/V \tag{2}$$

Q is utilized to denote the amount of charge stored on the electrode per unit mass, area, or volume. This charge storage capacity is an essential characteristic that determines the overall performance of a supercapacitor. On the other hand, V represents the operating voltage window, which refers to the range of voltages within which the supercapacitor can operate effectively. The operating voltage window is a critical parameter that defines the maximum and minimum voltages that can be applied to the supercapacitor without compromising its performance and safety. It is important to note that each material has its unique capacitance value. Therefore, it becomes necessary to utilize equation (3) to calculate the theoretical capacitance [61–63]:

$$C = (nFM)/V \tag{3}$$

n represents the number of electrons transferred during the redox reaction, specifically applicable to pseudocapacitive materials. F denotes the Faraday constant (9.648533212...×10^4 C), M signifies the molecular weight

of active material such as metal oxide for pseudocapacitor, and V represents the operating potential window. It is important to note that this equation is solely applicable to pseudocapacitor electrode materials owing to the involvement of the redox reaction. Therefore, the theoretical capacitance calculated using this equation is specific to pseudocapacitive systems [61–63].

2.3.1 EDLC (Electric Double Layer Capacitor)

The mechanism of the electric double layer takes place at the interface between the electrode and electrolyte in supercapacitors. This process involves the utilization of charged sites that store electrical charge. As a result, the charged sites at the electrode/electrolyte interface become temporarily diminished or consumed. The accumulation of electrons at the electrode surface is a non-Faradaic phenomenon. Figure 4 provides a schematic representation of the double-layer formation at the electrode/electrolyte interface, depicting both the Stern and the diffusion layer.

To attain a high capacitance in EDLCs, it is crucial to have an electrode material with excellent electrical conductance and greater surface area. The capacity improvement in EDLCs is directly linked to the efficient accumulation of ions at the interface between the electrode and electrolyte. The specific capacitance of EDLCs can be determined using the following equation (4) [61–63]:

$$C = \left(\varepsilon_r \varepsilon_o A\right)/d \tag{4}$$

where C is the specific capacitance, ε_r is the relative permittivity of the medium in the EDLC, ε_o is the vacuum permittivity, A is the surface area of the electrode, and d is the effective thickness of the electrical double-layer [61–63].

EDLCs mostly use carbon-based materials, such as graphite, graphene, reduced graphene oxide, graphene oxide, carbon nitride, carbon quantum dots, etc., due to their high surface area and porous quality. These materials offer superior both charge/discharge efficiency and cycle life. Nevertheless, they exhibit limitations concerning both specific capacitance and energy density [61–63].

2.3.2 Pseudocapacitors

The phenomenon observed is a consequence of the redox process occurring at the electrode-electrolyte interface. The accumulation of electrons at the electrode surface is a Faradaic process, involving the transfer of electrons generated by the redox reaction across the electrolyte-electrode interface. The current density associated with the faradaic processes flowing through the electrodes can be mathematically represented using equation (5) [61–63]:

$$C = \frac{nFd}{dt} dC_{ox} \tag{5}$$

n and F represent the number of electrons involved in the redox reaction and the Faraday constant, respectively. C_{ox} denotes the capacitance during the electrochemical process, and d signifies the thickness of the electrode material. Consequently, the overall current generated in the supercapacitor combines both the faradaic and non-faradaic currents, incorporating the contributions from double-layer capacitance and pseudo capacitance [61–63].

Figure 5 illustrates different mechanism types of the pseudosupercapacitor. The first mechanism, underpotential deposition (Fig. 5a), involves the reduction of metal cations to solid metal. These results in the deposition of metal species forming an adsorbed monolayer on the surface of a different

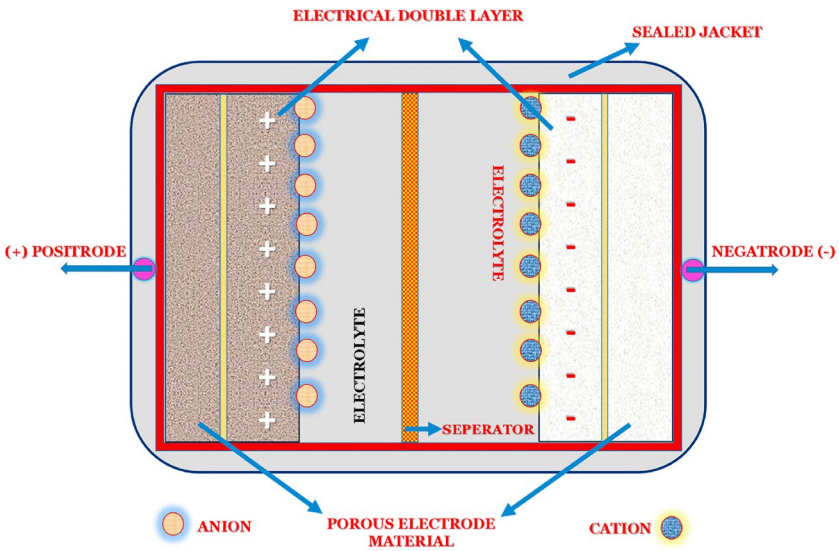


Fig. 4 Schematic concept of EDLCs. Copyright 2023, Elsevier. Reprinted with permission [64]

metal, leading to a lower negative potential compared to the equilibrium potential for metal reduction [65–67].

The second mechanism, redox pseudo capacitance (Fig. 5b), occurs when ions are electrochemically adsorbed onto near-surface materials, involving faradaic charge transfer. This mechanism is commonly observed in aqueous electrolytes and is seen in materials such as WO_3, nickel oxide (NiO), manganese oxide (MnO_2), cobalt oxide (Co_3O_4), ruthenium oxide (RuO_2), and conducting polymers [64].

Yao et al. provided an explanation for the charge storage mechanism of WO_3 electrode, suggesting the involvement of the following redox reaction:

$$\mathbf{WO_3 + xH^+ + xe^- \leftrightarrow H_xWO_3}$$

pseudocapacitive redox reaction mechanism of synthesized hierarchical WO_3 nanofibers on a flexible carbon cloth (CC) by a facile hydrothermal method [68]. Intercalation pseudocapacitance, as shown in Fig. 5c, is a widely used approach in non-aqueous electrolytes where ion diffusion into bulk phase host materials is kinetically controlled. In this process, ions intercalate into the tunnels or layers of the bulk material without causing any alteration in the crystallographic phase [64].

Metal oxides, metal nitrides, metal sulphides, metal hydroxides, and conducting polymers are commonly utilized electrode materials for pseudo capacitive behaviour. These materials are favoured due to their ability to exhibit different charge storage mechanism. PCs materials exhibit a notable specific capacity, providing considerable high power density and energy density. However, their values of rate capability are relatively lower as compared with other materials. The total capacitance of a system is determined by the combined contributions both of the pseudocapacitive capacitance, C_{pc} and the double-layer capacitance, C_{dl} [61–63].

$$C_T = C_{dl} + C_{pc} \tag{6}$$

2.3.3 Hybrid supercapacitors

A hybrid supercapacitor (Fig. 6) is a type of supercapacitors, integrates both the EDLCs mechanism and the PCs (redox) mechanism for energy storage. These devices can be constructed using diverse materials, such as, transition metal based compounds, conducting polymers and carbon-based materials [61–63].

Hybrid supercapacitors can be classified into three types: asymmetric, symmetric composite, and battery-like configurations.

Asymmetric hybrid supercapacitor The asymmetric hybrid supercapacitor consists of an anode made of metal based materials or conducting polymers, facilitating the PCs features. Conversely, the cathode can be carbon-based materials, enabling EDLC process. Such configuration offers notable advantages, including high energy density with the rapid discharge capabilities of capacitors, suitable for applications requiring quick energy boosts and higher storage, high power density, and exceptional cyclability [61–63]. Despite their advantages, their complexity and the materials used can increase costs and manufacturing challenges [34, 69]. For example, Patil et al. fabricated the flexible asymmetric device using WO_3 thin film as a negative electrode, polyaniline (PANI) as a positive electrode and polymer gel polyvinyl alcohol-sulfuric acid (PVA-H_2SO_4) as an electrolyte. The fabricated WO_3/PVA-H_2SO_4/PANI device showed a specific capacitance of 484 F/g with energy and power density of 113.7 Wh/kg and 1.1 kW/kg, respectively with

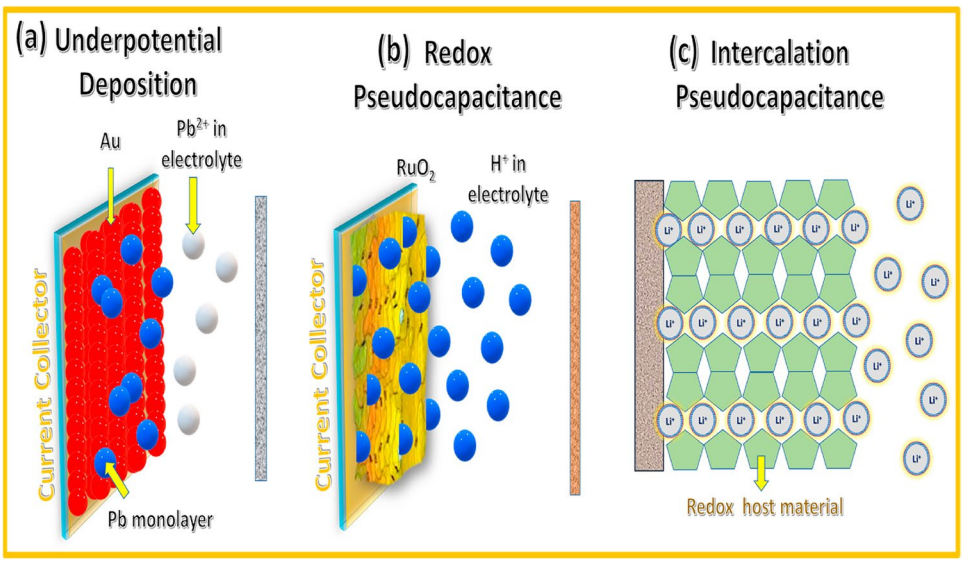


Fig. 5 Different working mechanisms of the pseudosupercapacitor (**a**) under potential (**b**) redox pseudocapacitance (**c**) intercalation. Copyright 2023, Elsevier. Reprinted with permission [64]

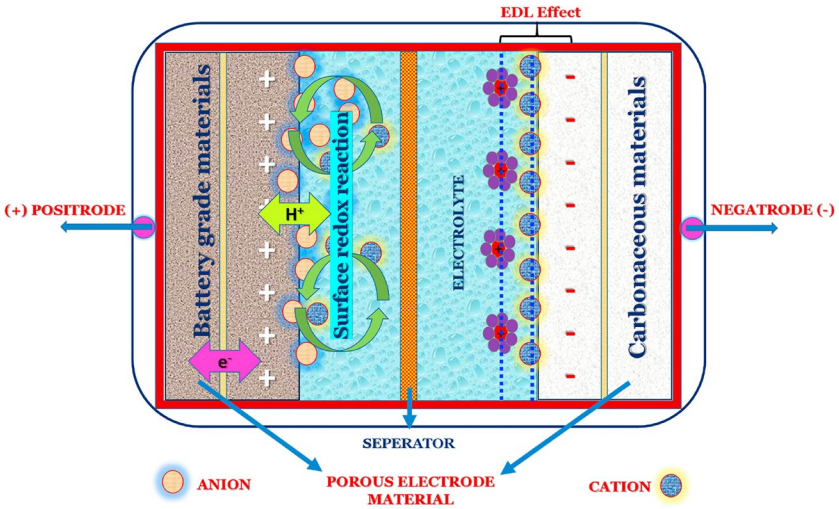


Fig. 6 Schematic mechanism of hybrid supercapacitor. Copyright 2023, Elsevier. Reprinted with permission [64]

85 % capacitive retention over 4000 CV cycles in applied potential window of +1.3 [70].

Symmetric hybrid supercapacitor The symmetric composite hybrid supercapacitor integrates both the anode and the cathode into a composite structure, offers simplicity, stability, and cost-effectiveness, excelling in applications where reliability over numerous cycles is paramount. It combines transition metal compounds, conducting polymers or carbon-based materials. This configuration leverages a combination of energy storage applications, encompassing both Faradaic and non-Faradaic reactions [61–63]. However, such type of supercapacitor stores less energy than asymmetric supercapacitors and have a narrow voltage range [71]. Men et al. prepared the WO_3@PANI composite flexible film as the electrode of the electrochromic supercapacitor by the continuous ionic layer adsorption reaction method and designed WO_3@PANI/H_2SO_4/WO_3@PANI symmetric supercapacitor. The designed device showed that the specific capacitance of electrochromic supercapacitor is 46.27 mF/cm^2, and the capacitance retention rate is 85 % after 3000 charge–discharge cycles [72].

Battery-like hybrid supercapacitor The battery-like hybrid supercapacitor features a cathode comprising carbon-based materials, which facilitates the EDLC process. On the other hand, the anode relies on a lithiation/de-lithiation involving Li^+ insertion during charging and Li^+ transfer during discharging. The preferred choice for the anode material is Li-rich, and the electrolyte must contain Li^+. This configuration provides high energy density but comes at a higher cost and requires careful matching of electrode capacities. The mass ratio of the (−) and (+) electrodes is adjusted to ensure capacity matching, following $Q^+ = Q^-$. This principle enables optimal electrochemical performance, described by equation (7). Selection of an appropriate electrolyte plays a crucial role in enhancing ion diffusion and increasing charge capacity [61–63].

$$\frac{m^+}{m^-} = \frac{(C^- \times \Delta V^-)}{(C^+ \times \Delta V^+)} \tag{7}$$

Battery-type hybrid supercapacitors are potential candidates for long-lasting power supplies compared with the conventional supercapacitor electrodes, but a major hurdle lies in the charge balancing of the two electrodes [73]. In addition, their downside includes a shorter lifespan compared to other supercapacitors and higher costs due to specialized materials [74].

Velmurugan et al. fabricated high crystalline WO_3 || Vanadium pentoxide (V_2O_5) thin film battery like where WO_3 and V_2O_5 showed pseudo-capacitive and battery-type behaviour, respectively [75].

2.4 Characteristics for the electrochemical performance of the supercapacitor electrodes

The evaluation of specific parameters related to capacitive behaviour plays a crucial role in characterizing supercapacitors and whose parameters include specific capacity, energy and power densities, coulombic efficiency, cycle stability, internal resistance, relaxation time, effective capacitance, and irreversible resistivity. These parameters are typically determined by applying three primary techniques: Cyclic Voltammetry (CV), Galvanostatic Charge-Discharge (GCD), and Electrochemical Impedance Spectroscopy (EIS) [63, 76]. These analyses can be performed using two or three electrochemical cell configurations [77]. It is important to determine these parameters accurately as they help in understanding the electrochemical performance of the capacitor and aid in designing efficient and reliable energy storage devices.

2.4.1 Cyclic Voltammetry (CV)

CV is a widely used electrochemical method involves the application of a periodically and linearly changing electric field to the electrodes. Once the desired potential is reached, the potential ramp at the working electrode is reversed. The current generated at the working electrode is graphed as regards the operating voltage, creating a CV graph that demonstrates the correlation between current and voltage. Examining the redox behaviour within the designated potential range is essential for assessing the measurement's efficacy. Conducting both forward and back forward scans is crucial to identify anodic and cathodic peaks associated with the electrode's charge and discharge processes. Furthermore, the choice of potential range for CV analysis is contingent upon the specific combination of electrolyte salt, solvent, and active material utilized in the working electrode [76].

Integrating the electric current over time provides valuable information about the accumulated charge at the electrode surface. The capacitance value can be estimated by dividing the accumulated charge by the potential range [76, 78].

The CV exhibits a distinct rectangular shape in ideal supercapacitors having minimal resistance, influenced by the scan rate (Fig. 7a). However, real capacitors deviate from this ideal shape owing to internal resistance, resulting in a modified CV (Fig. 7b). Pseudocapacitors exhibit the existence of redox peaks within the CV, indicating the involvement of redox reactions (Fig. 7c) [76, 78].

To differentiate between the charge storage mechanisms of supercapacitors and batteries (Fig. 8a and b), thus the CV technique provides valuable insights. In the CV graph of a supercapacitor, an ideal rectangular behaviour is observed, indicating the characteristic charge storage mechanism. On the other hand, the CV graph of a battery exhibits cathodic and anodic peaks, signifying the redox reactions occurring within the battery at specific potentials. It is noteworthy that the energy storage mechanism of an EDLC is independent of the applied voltage. Unlike an EDLC, the behaviour of a battery is strongly influenced by the applied potential, leading to variations in the peaks. Therefore, the detection of the applied voltage window for the battery in CV analysis is crucial for effectively investigating its energy storage behaviour [76, 77].

2.4.2 Galvanostatic Charge–Discharge (GCD)

GCD, an electrochemical method, is utilized to establish the capacitance electrochemically under constant current conditions, offering reliable results. Unlike CV, which varies the potential, GCD maintains a constant current while measuring the corresponding potential over time. This technique is highly effective in evaluating capacitance [77].

In the case of EDLCs, the potential window for charge storage is not dependent on the specific material. However, for redox-active and intercalated pseudocapacitors, such as flexible WO_3 electrodes, charge storage is influenced by the fixed potential range associated with the material [79].

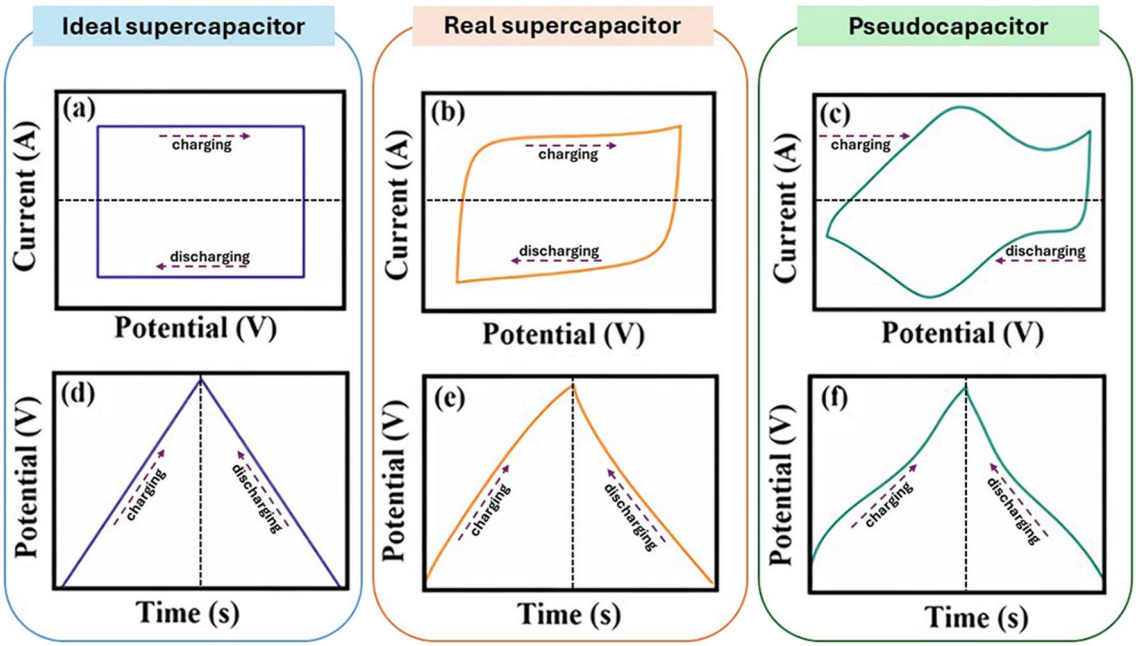


Fig. 7 CVs of (**a**) ideal supercapacitor (**b**) real supercapacitor (**c**) pseudocapacitor, and GCDs of (**d**) ideal supercapacitor (**e**) real supercapacitor (**f**) pseudocapacitor. Copyright 2020, Springer. Reproduced with permission [76]

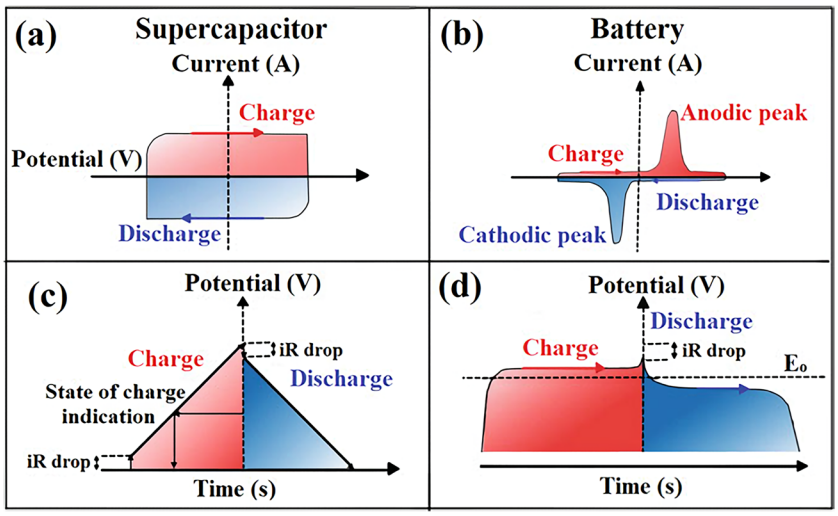


Fig. 8 (**a**, **b**) CV graphs of and (**c**, **d**) GCD graphs of supercapacitors and a batteries. Copyright 2020, Springer. Reprinted with permission [76]

Figure 7d, e and f depict typical GCD curves for ideal capacitors, real capacitors, and pseudocapacitors, respectively. Ideal capacitors exhibit perfect linear behaviour, while real capacitors and pseudocapacitors display redox peaks. GCD can be applied in various settings, including laboratories and industries, providing valuable information on cell capacitance, resistance, and cyclic stability [76, 78].

To gain further insights into GCD behaviour in energy storage devices, Figure 8c and d depict typical GCD curves for pseudocapacitors. The linear charge-discharge curve observed in EDLCs represents ideal capacitive behaviour with no redox peaks. In contrast, batteries display a charge/discharge plateau at a consistent voltage. The initial slight potential drop observed in the GCD is attributed to the equivalent series resistance of the supercapacitor [76, 78].

2.4.3 Electrochemical Impedance Spectroscopy (EIS)

EIS is a commonly employed technique to investigate the impedance characteristics of a system under alternating current conditions. It involves measuring the impedance of an equivalent circuit consisting of different electrical components connected in series and parallel configurations, such as resistance, impedance, and inductance. The frequency response characteristics can be analysed to gain insights into electrochemical capacitors with non-conductive/reactive electrodes or electroactive electrodes by conducting measurements at various frequencies. This analysis provides valuable information about the intrinsic properties of the electrode material, porosity distribution in extensive surface area electrodes, and characteristics like particle-particle interaction and thickness of the electrode material [76, 77, 80].

EIS spectra are particularly relevant for studying capacitive behaviour as they directly reveal the capacitance component of the impedance, denoted as $1/j\omega C$. The frequency response behaviour enables the observation of the role played by the porous electrode. The real and imaginary components of impedance help distinguish the pseudocapacitive behaviour exhibited by a supercapacitor [76, 77, 80].

The Nyquist plot is a powerful tool for analysing a real capacitor, featuring an additional semicircle that represents the parallel combination of bulk resistance (related to ion movement) and geometric capacitance (arising from the dielectric polarization of the electrolyte at the applied voltage). While extracting this plot electrochemically, this provides crucial information about the specific capacity, energy and power densities of the supercapacitor. These metrics are crucial for evaluating the super capacitive performance of both the electrode material and the integrated cell device. Figure 9a schematically illustrates the Nyquist plot, while Fig. 9b shows the corresponding Bode phase. Figure 9 demonstrates the typical impedance behaviour, characterized by three essential sites: a high-frequency semicircle, mid-frequency Warburg impedance, and low-frequency capacitive behaviour [76, 77, 80].

2.5 Electrical parameters evaluation for supercapacitors

2.5.1 Capacitance

The capacitance of a supercapacitor is determined by the presence of two capacitances connected in series, which are formed at the electrode-electrolyte contact region. Each electrode in a supercapacitor is denoted as C_1 and C_2, contributing to the total capacitance, C_T, according to the equation [81]:

$$\frac{1}{C_T} = \frac{1}{C_1} + \frac{1}{C_2} \tag{8}$$

جامعة قطر QATAR UNIVERSITY

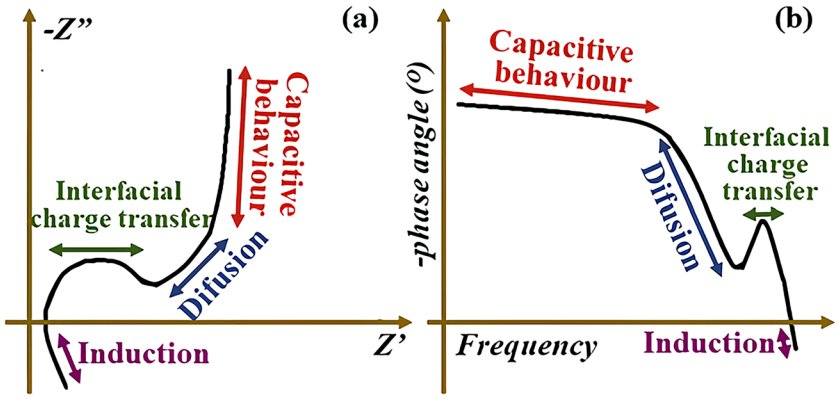


Fig. 9 Schematic representation of an impedance model: (**a**) Nyquist plot and (**b**) Bode plot. Copyright 2020, Springer. Reprinted with permission [76]

In symmetric supercapacitors where $C_1 = C_2$, the sum of capacitance is half the capacitance of either electrode. In asymmetric systems, C_T is primarily influenced by the electrode with the lower capacitance. The evaluation of supercapacitor capacitance can be carried out using the GCD and CV analyses. The capacitance value obtained from CV is determined using the equation [81]:

$$C_{cv} = \int \frac{Idu}{2vm\Delta V} \tag{9}$$

ν denotes the scan rate, m indicates the mass of the active material of the electrode, ΔV represents the applied potential window, and I represents the constant current [81].

In GCD, the capacitance can be determined using the equation:

$$C_{GCD} = \frac{I\Delta t}{m\Delta V} \tag{10}$$

In this equation, m denotes the mass of the active material of the electrode, ΔV corresponds to the discharge voltage, Δt indicates the discharge time, and I represents the constant current [76, 77, 81].

The capacitance of the electrodes, normalized by their respective areas, is determined by analysing the GCD and CV techniques. The calculation is performed as follows [77, 81, 82].

$$C_{GCD,\ areal} = C_{GCD}\rho \tag{11}$$

Here, ρ represents the weight of the active material per cm square. The complex capacitance, which characterizes the frequency-dependent behaviour, is determined through EIS [77, 82]:

$$C * = C' - iC' \tag{12}$$

$$C' = \frac{Z''}{\omega|Z|^2} \tag{13}$$

$$C'' = \frac{Z'}{\omega|Z|^2} \tag{14}$$

In the provided equation, the symbol ω represents 2π times the frequency. The relaxation time, τ is defined as the inverse of the relaxation frequencies that correspond to the peaks of the imaginary part of the capacitance, C'' [77, 82].

2.5.2 Reducing Equivalent Series Resistance (ESR)

Reducing the equivalent series resistance (ESR) is widely recognized as a critical factor in enhancing power density. ESR encompasses a range of resistances within a supercapacitor system. These include the internal resistance of the electrode and electrolyte, the charge transfer resistance of electrolytic ions and the contact resistance between different components of the supercapacitor. By considering these resistances, one can better understand the total performance and efficiency of the supercapacitor. To optimize power density, it is favourable to employ an electrolyte with high ionic conductivity and a wide potential window [76, 77].

Different electrolyte types exhibit varying conductivity and potential window characteristics. For instance, aqueous electrolytes offer high conductivity but have a narrow potential window. On the other hand, organic electrolytes and ionic liquids provide a wider potential window but exhibit lower ionic conductivity, resulting in higher ESR and lowering power density [76, 77].

The GCD analysis is utilized to measure the resistance of the supercapacitor. During the transition from the charge to discharge, directly voltage drop is determined, as depicted in Fig. 8c and d. The measurement of ESR involves determining the iR drop by plotting current density versus the corresponding voltage drop calculated at various current densities. The iR drop is determined using the equation [77, 81]:

$$iR_{drop} = a + bI \tag{15}$$

a represents the voltage difference between the applied voltage and the actual voltage, while *b* corresponds to twice the value of ESR [77, 81].

2.5.3 Energy density and power density

Energy density, *E* of a charged supercapacitor is determined by the applied potential window *(ΔV)* and the capacity (C_r) of the supercapacitor. This parameter is determined from the GCD using the following formula [76, 77]:

$$E = \frac{1}{2} C_r (\Delta V)^2 \tag{16}$$

Power density, *P* represents the energy output per unit of time *(Δt)* and indicates how quickly a supercapacitor can deliver charge to an external load. It is determined from the GCD by using the following formula [76, 77]:

$$P = \frac{E}{\Delta t} \tag{17}$$

Alternatively, power density can be calculated using the following equation [76, 77]:

$$P = \frac{\Delta V^2}{4R_S} \tag{18}$$

The parameters *V* (cell voltage), C_T (total capacitance), and R_S (equivalent series resistance) play a crucial role to enhance the energy and power densities of supercapacitors. Increasing *V* and C_T while simultaneously reducing R_S can contribute to the development of high-performance supercapacitors [76, 77].

2.5.4 Cycle stability

The stability of a supercapacitor is an significant performance parameter. CV and GCD tests are conducted over numerous cycles to assess the stability of the material of electrode in half-cell or the full-cell configurations. Carbon-based electrode materials demonstrate excellent cyclic stability due to their physical charge storage mechanism, enabling highly reversible charge-discharge processes. In contrast, pseudocapacitive electrode materials exhibit poor cyclic stability due to the involvement of chemical processes that reduce the reversibility of the electrode material. The cyclic performance of supercapacitors are influenced by various factors, such as charge-discharge rate, the types of electrode material and electrolyte, applied voltage range, and thermal conditions. These factors collectively characterize the supercapacitor's ability to maintain stable performance over repeated charge-discharge cycles [76, 77].

2.5.5 Columbic efficiency

Coulombic efficiency, a crucial performance metric in supercapacitor applications, quantifies the ratio of energy consumed during the charging process to the energy discharged by the device. This efficiency parameter is derived from the GCD by evaluating the ratio of discharge time to charge time, expressed as a percentage (19) [83].

$$\text{Coulombic efficiency}, \% = \frac{\text{Discharge time}}{\text{charge time}} \times 100 \tag{19}$$

2.5.6 Internal discharge rate

Internal discharge describes the lowering of potential in a charged device over time. It primarily occurs due to current leakage in the charged electrode, leading to a decline in cell voltage. The higher internal discharge rates, the more it can restrict the practical use of supercapacitor performance electrochemically [84].

2.5.7 Thermal stability

Supercapacitors provide a broader operating temperature range as compared with battery technologies. The performance of supercapacitors at different temperatures is influenced by several factors, including species of electrolyte and electrode material exploited, as well as the stability of the separator and current collector under specific operating thermal conditions [47, 76].

3 Flexible WO_3 based electrodes in supercapacitors

3.1 Fabrication of the flexible WO_3 based electrodes

WO_3 has been one of the most widely studied TMOs due to its semiconducting properties and propensity to accommodate small intercalating cations [85]. Production of the WO_3-based electrodes are very important for the final performance of energy storage systems [86]. The contact between the active material and the substrate plays a key role in electrode preparation due to the energy storage mechanism activated by an electric field. Here, the most used procedure for WO_3 electrode preparation is reported. Copper (Cu) [87], stainless steel mesh [88], titanium foil [89], carbon-based substrates [90], and fluorine tin oxide (FTO) coated glass [91] are most commonly used substrates.

Various methods can be employed to produce WO_3-based electrodes with control over electrical conductivity, morphology, crystallographic structure, bandgap, and surface area. These methods include direct synthesis of the active materials onto the substrate surface and the deposition of a homogeneous WO_3-based slurry using techniques such as drop casting or spin coating. In the WO_3-based slurry, a conductive material and a binder is mixed with WO_3 nanostructures. Nafion, polytetrafluoroethylene or poly(vinylidene fluoride) have been used as binders. For homogeneity, different solvents are also added to WO_3-based slurry [92]. Using the process, a large scale can be obtained for industrial applications. There are many works in literatures. WO_3-based slurry electrode onto carbon substrate was obtained using drop casting process [93]. Despite many efforts for slurry electrode, the adhesion of WO_3 materials on to substrate is still a problem. Non-uniform electrodes can result fragmentation, restack, re-aggregation and instability situations. Alternative method as a solution to this problem is to prepare electrode by growing WO_3 material on the substrate. One highly effective strategy for the direct growth of WO_3 nanoarrays on transparent conductive substrates is attributed to several factors, including short ion transport paths, high surface area, direct electron transport pathway, numerous electroactive sites, and superior permeability.

3.1.1 Chemical/Physical vapor deposition

Chemical/physical vapor deposition (CVD/PVD) is one of the most used techniques for thin film deposition. The system consists of a deposition chamber, evaporation source and target material. Using these methods, it is possible to obtain ultrathin 2D nanofilms using vapours or liquids. The methods are useful for layer or non-layered WO_3 precursors [94]. Although these techniques provide higher quality products, they require very high costs due to an inert atmosphere, high-temperature conditions. Atomic layer deposition is similar process to PVD synthesis technique. It is capable to obtain materials high quality thin films in different compositions [95]. Figure 10 shows an evaporation deposition setup [96].

3.1.2 Solvothermal and hydrothermal synthesis

WO_3-based materials can be produced controlling as layered and non-layered nano-sheets also with solvothermal and hydrothermal synthesis process [98]. Solvothermal synthesis is a non-aqueous solvent-driven synthesis while hydrothermal synthesis is an aqueous medium [99]. The solvo/hydrothermal synthesis provides layered and non-layered WO_3 nano sheets which have high yield and tunable thickness. This process needs some special conditions to obtain the desired product due to uncontrollable parameters. Figure 11 shows the design procedure for hexagonal branched nanowire WO_3/FTO electrode [100].

The key distinction between the solvothermal and hydrothermal methods lies in the choice of process solvent. Hydrothermal methods exclusively utilize water as the solvent. In contrast, solvothermal processes offer greater flexibility, allowing the use of pure organic substances, combinations of organic materials, or mixtures of water and organic solvents as the solvent. In that paper, WO_3 nano-grass blades were synthesized on an FTO substrate utilizing the solvothermal method [101].

3.1.3 Pulsed Laser Deposition (PLD)

PLD is a process which is not restrictions on target material (Fig. 12). WO_3 films can be obtained in 10-500 nm thickness on different substrate electrodes [102]. PLD stands as a cutting-edge technique capable of generating diverse material morphologies. This method is instrumental in producing electrodes with exceptional electrochemical performance.

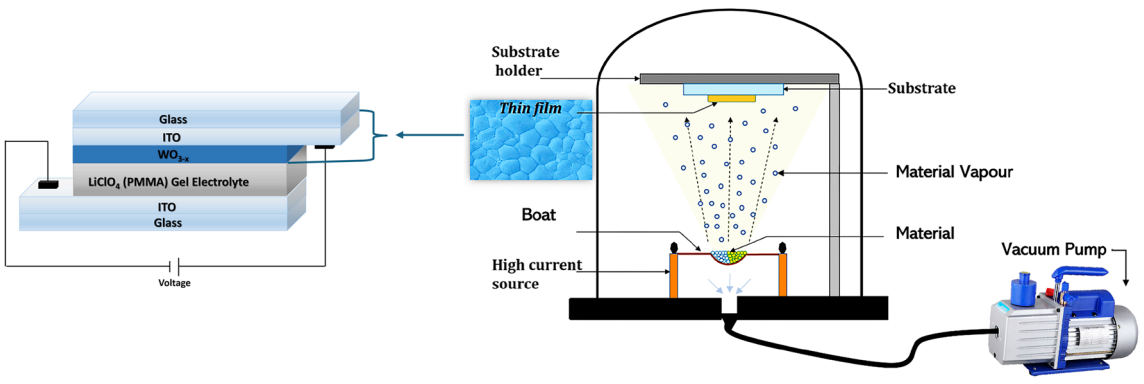


Fig. 10 Schematic illustration of the PVD setup and design of the symmetric device of the flexible WO_3 thin film electrode for supercapacitor performance estimation analyses. Copyright 2019, Elsevier and Copyright 2023, American Chemical Society and Reproduced with permissions [96, 97]

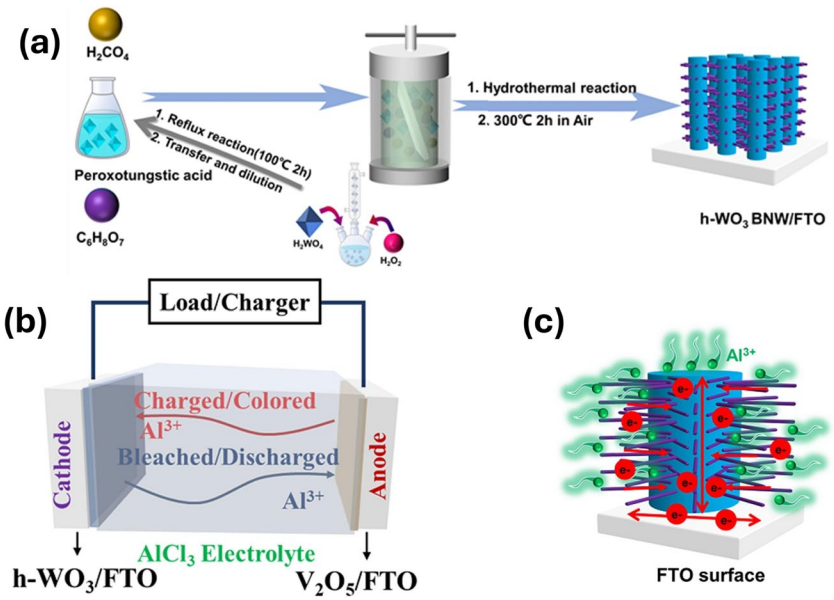


Fig. 11 The design procedure for hexagonal branched nanowire WO_3/FTO electrode: (**a**) fabrication procedure of the flexible thin film electrode, (**b**) its asymmetric supercapacitor (ASC) device, (**c**) electrochemical reaction mechanism. Copyright 2022, Elsevier. Reproduced with permission [100]

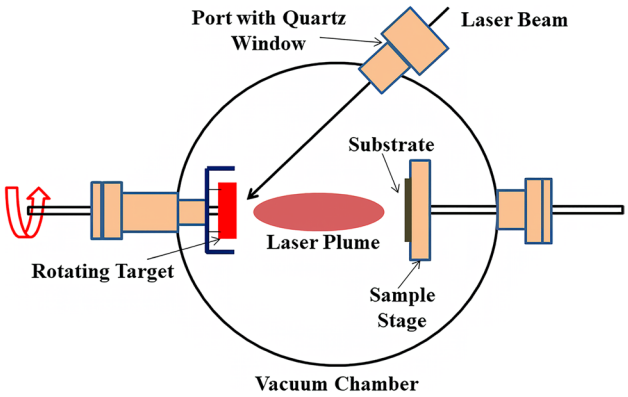


Fig. 12 Diagram of PLD setup. Copyright 2019, Elsevier. Reprinted with permission [102]

In contrast to traditional thin film fabrication methods, where adjusting substrate temperature is necessary to modify film properties, PLD offers an additional dimension: the ability to alter the film texture by modulating the energy of the ablated particles.

PLD plays a crucial role in fabrication of flexible electrode fabrication for supercapacitor. This process provides tunable nanostructures, well and fine thin film thickness in regulated chemical composites [75]. Co_3O_4 &WO_3 thin films were also obtained using PLD varying pulsed repetition rates for flexible supercapacitor device (Fig. 13) [103].

3.1.4 Electrochemical anodization and electrodeposition

Electrochemical anodization and electrodeposition are another electrode production techniques. Electrochemical anodization is useful technique to obtain oxide film, to change surface colour, to enhance corrosion resistance, to protect metal surface on the metal surface by using the valve metal as anode during electrolysis.

In electrodeposition process, the cathode is working electrode which has transport electron from plating solution during electrodeposition. W element has formed as WO_x thin film on the cathode. WO_3 film on the FTO glass substrate was synthesized via the facile electrodeposition method at room temperature by Poongodi et al. [104].

Hepel et al. synthesized rGO (reduced graphene oxide)/WO_3 films by electrochemical nucleation and growth using pertungstic acid [105]. Dadashi et al. prepared PANI-WO_3 nanocomposite onto anodized graphene oxide nanosheets (PANI-WO_3/GO NSs)/graphite electrode by pulse reverse co-electrodeposition of PANI and WO_3 nanocomposite onto earlier anodized graphene oxide nanosheets/graphite electrode (Fig. 14) [106]. The PANI-WO_3/GO nanosheets/graphite electrode was obtained, exhibiting superior mechanical strength, excellent wettability, low ohmic drop, small charge transfer resistance, and an outstanding specific capacitance of 677 F/g, making it highly suitable for supercapacitor applications.

3.1.5 Sol-gel process and Self-assembly synthesis

Sol-gel is a widely used process in the field of wet chemical process for WO_3 films. The sol is the precursor solution and the sol-gel are dip-coated, drop-cast or spin coated onto the substrate to obtain a WO_3 film. Incorporating the sol-gel process for synthesizing WO_3 flexible thin films offers significant advantages, including lower processing temperatures essential for flexible substrates, ensuring homogeneity and consistent properties across electrodes. This method's cost-effectiveness and precise control over film composition are key benefits. By

جامعة قطر QATAR UNIVERSITY

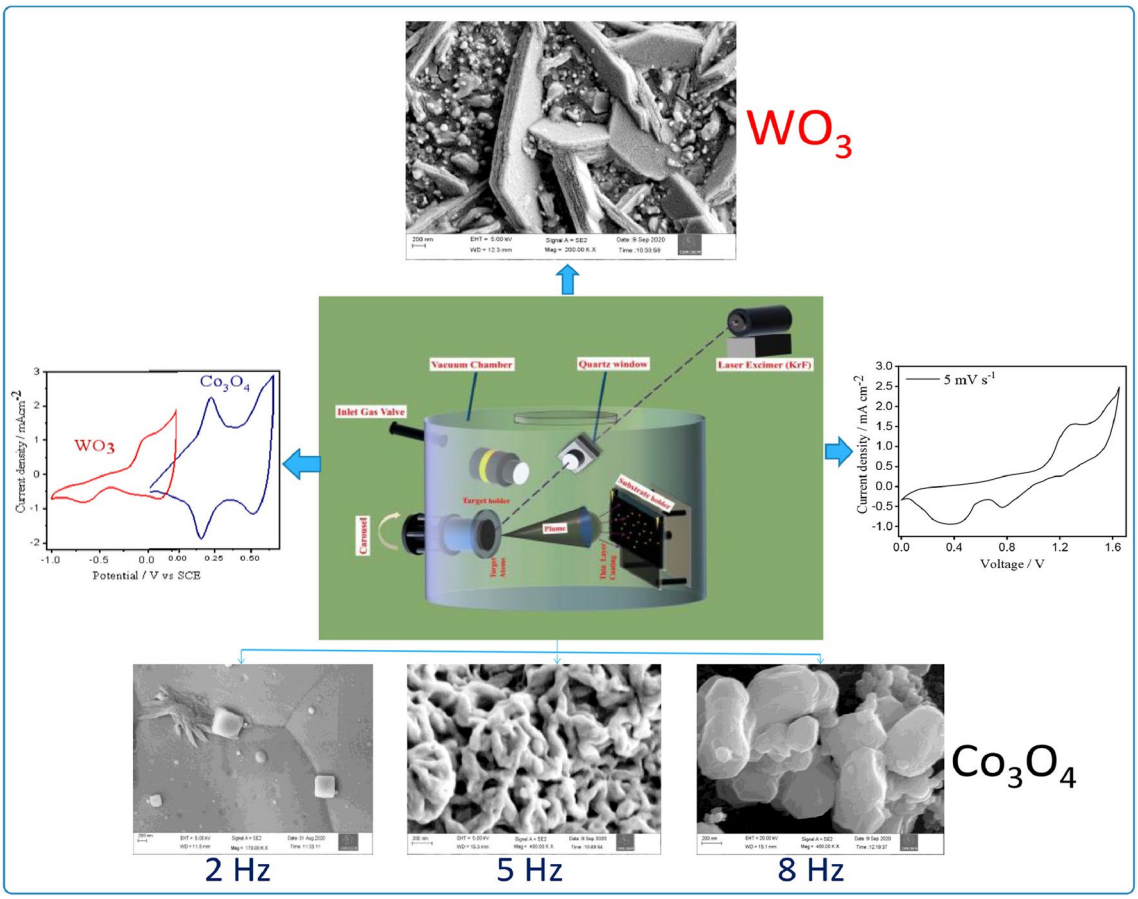


Fig. 13 Schematic representation of PLD coating of Co_3O_4 & WO_3 thin films. Copyright 2022, Elsevier. Reprinted with permission [103]

employing doping strategies, such as the addition of elements like nitrogen or carbon, and combining methods like electrodeposition or templating while adjusting process parameters, the electrochemical properties, surface area, and structural features of WO_3 films can be significantly enhanced [107, 108]. Such improvements are instrumental in augmenting the conductivity, capacitance, mechanical resilience, and longevity of electrodes, aspects that are essential for their application in supercapacitors. Highlighting this, Nguyen et al. demonstrated that using polyethylene glycol as a structure-directing agent in the sol-gel process can modify the porosity and composition of WO_3, leading to films with microporous networks

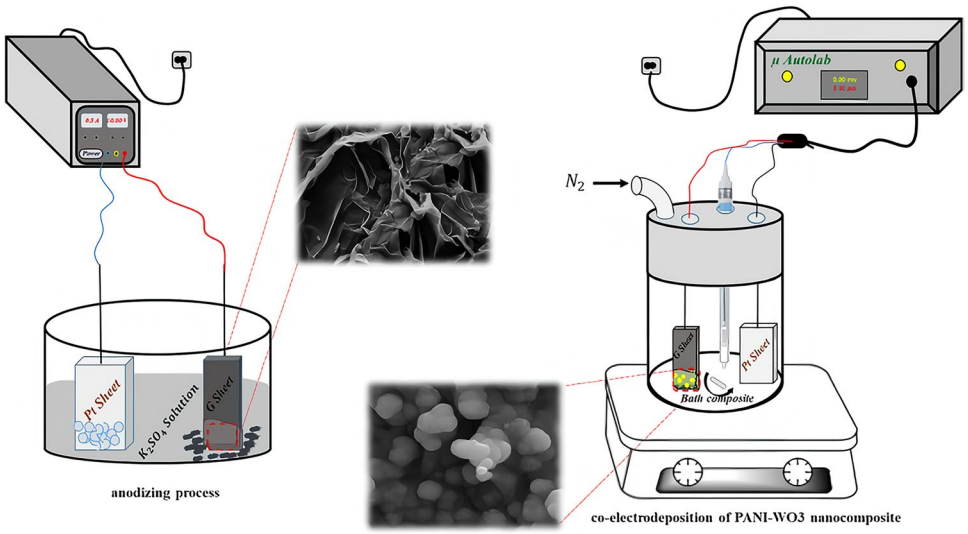


Fig. 14 Design of PANI-WO_3/GO NSs/graphite electrode process. Copyright 2023, Springer. Reprinted with permission [106]

that facilitate fast reversible electrochromic switching—an advantageous feature for supercapacitors due to improved ion transport and storage capabilities [109].

The other wet chemistry is the self-assembly synthesis method for large-scale production in industries [100]. Following the self-assembly process, the material is subjected to hydrothermal or solvothermal treatment. This treatment involves exposing the material to high temperatures and pressures in a liquid environment. The purpose of this treatment is to induce condensation and crystallization, allowing the material to form a more stable and structured configuration. Additionally, during this process, the surfactant, which was initially used to facilitate self-assembly, is removed. This step is crucial as it helps eliminate any residual surfactant and further enhances the material's properties and performance. Mesoporous metal oxides were prepared by evaporation-induced self-assembly method combining sol-gel chemistry and molecular self-assembly for electrochromic supercapacitor [110].

3.2 Electrochemical performance of WO_3-based electrodes for flexible supercapacitor applications

3.2.1 WO_3 for flexible supercapacitors

Diverse TMOs including RuO_2, MnO_2 have been commonly surveyed as pseudocapacitive materials to increase the supercapacitor performance. Although, most of these were utilized as cathode materials, the anode material's performance also should be advanced for attaining maximum energy density of full device [21]. Recently, WO_3 has been widely investigated as anode materials for supercapacitor applications, because of its high theoretical capacity, environmental friendliness and cheaper [88, 89]. Indeed, WO_3 is considered an n-type semiconductor characterized by a wide bandgap falling within the range of 2.5-3.5 eV. The specific value of the band gap varies based on the degree of distortion from its cubic structure and its state, be it crystalline or amorphous. It gained much attention due to its advantage features such as its adjustable crystal structures, low cost, non-toxicity and broadly favourable in the diversified forms [111, 112]. Tungsten oxides with diverse valence states (6^+, 5^+, 4^+, 3^+) possess considerable physical and chemical features with diverse negative potential ranges (~ −0.8 V) in acidic and neutral mediums, which have a significant act for elevated energy density. Elevated power capability and fast charging time do tungsten trioxides with diverse valence states turn into a considerable candidate for electrode materials [113].

Numerous techniques have been employed to enhance the performance of WO_3 and broaden its applications. One such method involves introducing dopants into its lattice to adjust and enhance its features for specific applications. Various types of dopants, including anions, cations, and unstable dopants, have been studied for their influence on the structural, optical, electronic, and magnetic properties of WO_3 [114].

Among these dopants, intrinsic oxygen vacancies play a significant role in improving the performance of WO_3. Electrodes of WO_3-δ with controlled oxygen vacancy concentrations have demonstrated improved electrical conductivities. This enhancement results in lower equivalent series resistance, reduced charge transfer resistance, and an enhanced current response. Consequently, these improvements allow for better electrochemical energy storage capacity [114].

Getting of higher capacitive performance of WO_3 can probably be by preparing WO_3 with suitable crystal form along with huge specific surface area [115]. WO_3 has five crystal structures as monoclinic ε-WO_3, triclinic δ-WO_3, orthorhombic β-WO_3, tetragonal α-WO_3, and hexagonal phases [115]. There was the impact of crystallinity on the supercapacitor performance. WO_3 having well-crystalline supply pseudocapacitance mainly relied on their capability to intercalate ions into the crystalline structure, which generally possess hassle contracting or expanding, and thus standing from the limited ion diffusion and penetration restraints, and considerably affecting their cycling durability and rate performance. WO_3 materials with low crystallinity or in an amorphous state often exhibit superior performance compared to their highly crystalline counterparts. This is because materials with more structural disorder and defects, characteristic of low-crystalline or amorphous states, tend to demonstrate enhanced properties [21].

Thin film based electrodes supply a significant contribution onto supercapacitor applications because of the direct grown onto substrates and free from binders and conductive additives that lead to improve supercapacitor characteristics including fast charge transfer rate, reducing path length based on electron transfer and superior durability [116]. This section discusses high-performance flexible supercapacitors developed in the past decade, focusing on those based on WO_3 and its hybrid composites.

3.2.2 WO_3 and its composites-based flexible supercapacitors devices

WO_3-based a flexible symmetric supercapacitor was produced by Mohan et al. The produced supercapacitor device had a specific capacitance of 64 F/g at 5 mV/s [117]. Karuppaiah et al. produced amorphous WO_3 based film onto flexible conductive polyethylene terephthalate (PET) film using radio frequency (RF) magnetron sputtering method. WO_3@PET-100 W samples owned an elevated areal capacitance of 9.76 mF/cm^2. Moreover, WO_3@PET//$LiClO_4$/PVA// WO_3@PET was assembled as solid-state symmetric supercapacitor device which exhibited pseudocapacitive behaviour with an energy density of 0.20 μWh/cm^2 and the power density of

150 μW/cm^2 [116]. Sun et al. presented novelty that WO_3@$W_{18}O_{49}$ doped flexible and conductive carbon nanofibers (CNFs) can be utilized as an electrode without any bonding agents and conductive compounds. WO_3@$W_{18}O_{49}$-CNFs displayed an elevated specific capacitance of 333.92 F/g and a significant cycling durability with capacitance retention of 98.12% after 5,000 cycles [113]. The generation of flexible WO_3 nanofibers on a flexible CC via a simple hydrothermal technique was reported by Yao et al. The as-prepared WO_3 fiber electrodes displayed elevated discharge areal capacitance (1716.92 mF/cm^2 at 2 mA/cm^2) and cycling durability (20.9% loss after 6,000 repetitive cycles at 10 mA/cm^2) [68].

Wu et al. deposited WO_3 nanotube bundles as the electrode materials on CC using a template- and surfactant-free hydrothermal process [20]. To evaluate potential application area in flexible supercapacitor of as-deposited electrode, electrochemical behaviour was investigated, as seen in Fig. 15. Redox peaks of WO_3 electrode were displayed at ~ −0.3 V, −0.43 V, which attributed to reversible intercalation/de-intercalation of H^+ ions into/out of WO_3 host. Areal capacitances of WO_3 nanotube bundles electrode was obtained as 2575.3, 2462.4, 2371.2, 2245.7, 2137.4 and 1985.2 mF/cm^2 at current densities of 3, 4, 5, 6, 8 and 10 mA/cm^2 , respectively. The specific capacitances were calculated to 643.9, 615.7, 592.8, 561.4, 534.2 and 496.4 F/g at current densities of 0.75, 1, 1.25, 1.5, 2 and 2.5 A/g, respectively. Repeating charge and discharge cycles were utilized at the current density 2.5 A/g for 6,000 cycle to evaluate durability of cycling performance. The electrochemical behaviour of redox species in the electrolyte was also evaluated using EIS technique. WO_3 nanotube bundle electrodes demonstrated enhanced conductivity with resistance of 0.79 Ω [20].

A study by Chen et al. carried out to better understand the impact of crystallinity on the electrochemical characteristic of WO_3 [100]. Low-crystalline WO_3 (LC-WO_3) and high-crystalline WO_3 (HC-WO_3) anode materials were fabricated using controlled the hydrothermal synthesis. The outputs demonstrated that because of more structural defects and disorders, LC-WO_3 exhibited faster redox reactions and capacitive-dominant energy storage feature, therefore supplying high capacitance performance (474 F/g) and increased performance of capacitance retention. By manufacturing a flexible solid-state asymmetry supercapacitor including LC-WO_3 electrode on porous CC, an energy density of 7.6 mWh/cm^3 and significant cycling durability with 92% capacitance retention after 10,000 cycles were obtained [21]. The electrochemical properties of WO_3 are significantly influenced by its various polymorphic forms, which are characterized by the arrangement of octahedral (WO_6) atoms at the corners and edges. One particular class of interest is the hydrated tungsten oxide ($WO_3.nH_2O$), where n represents different stoichiometric ratios such as 2, 1, 0.5, and 0.33. These hydrated forms exhibit unique arrays of distorted octahedral structures within their lattice, resulting in the generation of van der Waals gaps. These gaps are attributed to the regular confinement of water molecules (nH_2O) between the layers of the WO_3 structure. The presence of water molecules in the $WO_3.nH_2O$ introduces additional intercalation sites and influences the overall electrochemical behaviour, making it an intriguing material for supercapacitor applications [18]. Yin et al. reported that when compared to o the (002) and (020) facets, mesoporous WO_3 nanosheets with exposed (200) facets provide abundant adsorption sites for Na^+ in electrolyte, which expedites the Na^+ redox reaction kinetics for the enhanced supercapacitor performance. The electrochemical impedance spectroscopy of WO_3@ activated CC (ACC)-n (n=7, 8, 9) was carried out. At the low frequency, more vertical line was obtained for WO_3@ ACC-8, demonstrating a more ideal capacitive behaviour. The produced WO_3@ACC-8 electrode showed a high areal capacitance of 659 mF/cm^2, at a current density of 5 mA/cm^2 [22]. Gupta et al. presented a flexible quasi-solid-state hybrid supercapacitor design, which incorporated hydrated WO_3 nanorods as the negative electrode and exfoliated rGO as the positive electrode. This configuration exhibited remarkable electrochemical performance, with a high specific capacitance of 123 F/g achieved at a current density of 1 A/g. The supercapacitor also demonstrated excellent cyclic durability, retaining 92% of its initial capacitance after 2,000 cycles at a scan rate of 30 mV/s. These findings, as shown in Fig. 16, highlight the potential of this hybrid system for energy storage applications [18].

Some papers about WO_3 composite materials for hybrid supercapacitors were reported to provide fast charge/discharge, long-time cycling durability. Grafted WO_{3-x} nanoparticles-based micro-supercapacitors on rGO as the carbon support were produced to enhance the electrochemical double-layer capacitance of bare rGO with the addition of WO_{3-x} as great pseudocapacitance of the transition metal oxide. The rGO/WO_3 electrodes demonstrated the high volumetric capacitance of 56.5 F/cm^3, energy density of 12.2 mWh/cm^3, power density of 95 W/cm^3 [105]. Moreover, WO_3 with considerable pseudocapacitive behaviour exhibits elevated theoretical specific capacitance where carbon nanotubes (CNTs) with electrochemical double-layer capacitors exhibit significant electrical conductivity and enormous surface area [118]. Faraji et al. produced The multi-walled carbon nanotubes (MWCNTs)-WO_3-graphite sheet with flexibility and outstanding mechanical durability which showed perfect electrochemical behaviours with a low ohmic drop and an elevated areal capacitance of 114 mF/cm^2 (103 F/g) at 1.7 mA/cm^2 (1.5 A/g) in the presence of 1.0 M H_2SO_4 electrolyte [118]. The other significant way to increase the electronic and ionic features to mix it with other pseudocapacitive transition metal oxides. Shinde et al. synthesized WO_3-MnO_2

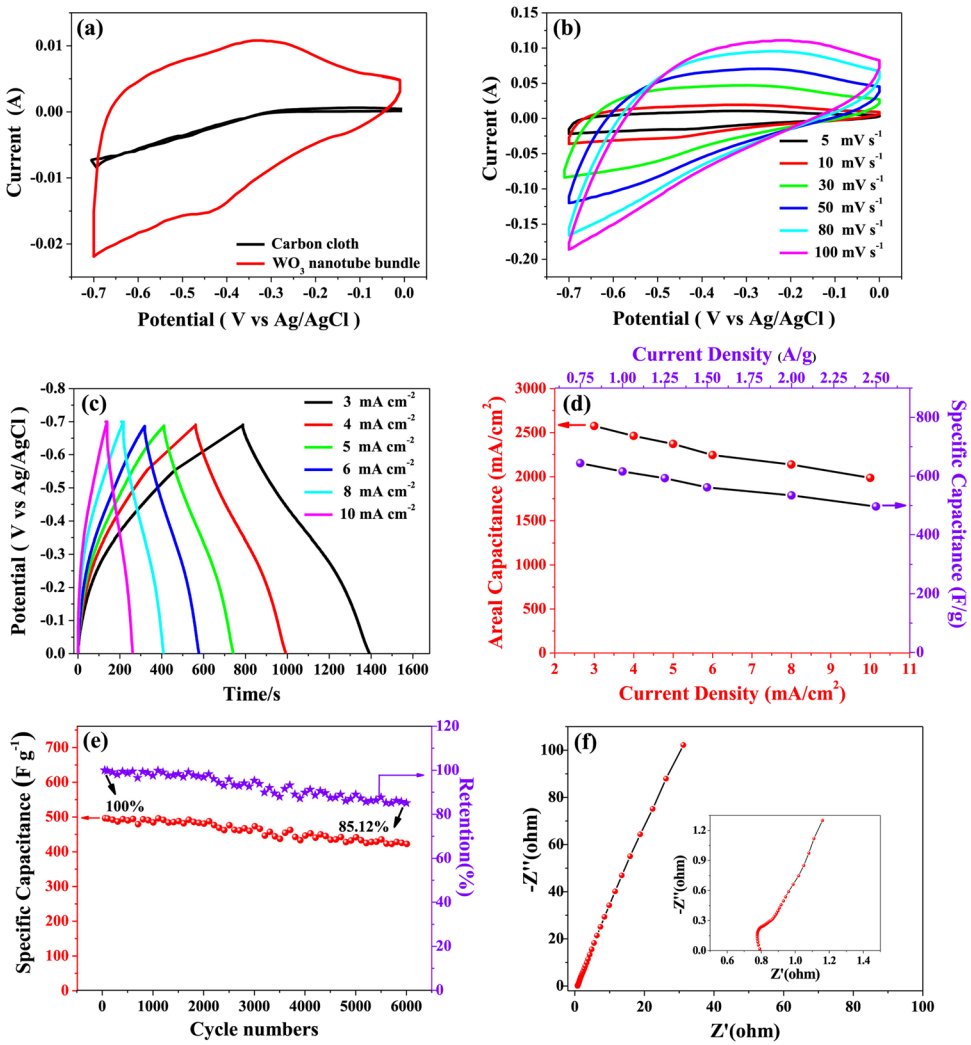


Fig. 15 Electrochemical characteristics of WO_3 nanotube bundle electrode: (**a**) Comparative CV curves between the as-synthesized WO_3 nanotube bundle and CC at a scan rate of 5 mV/s (**b**) CV curves obtained at various scan rates for the WO_3 nanotube bundle. (**c**) GCD curves recorded at different current densities. (**d**) Specific capacitance and areal capacitance of the resulting WO_3 products at varying current densities. (**e**) Cycling performance and capacitance retention of the WO_3 nanotube bundle electrode at a current density of 2.5 A/g. (**f**) Nyquist plot representing the impedance characteristics of the WO_3 nanotube bundle electrode. Copyright 2017, Elsevier. Reprinted with permission [20]

composite by hydrothermal technique and achieved superior specific capacitance of 609 F/g at, whereas WO_3 electrode was exhibited 413 F/g a scan rate of 5 mV/s [79]. Ju et al. was fabricated $Ti_3C_2T_x/WO_{3-x}$ nanocomposite using a solvothermal technique. Because of the synergistic influence of $Ti_3C_2T_x$ and WO_{3-x}, the fabricated nanocomposite electrode showed an enhanced capacity as 442 F/g at 2 mV/s and an elevated capacitance retention (75.8%) at 200 mV/s. When compared to $Ti_3C_2T_x$ electrode, the smaller equivalent series resistance and charge transfer resistance were attained. These results demonstrated perfect electron and ionic response, which belongs to the considerable rate capability of the nanocomposite electrode. In addition, the $Ti_3C_2T_x/WO_{3-x}$ composites demonstrated 91.21% capacity retention after 10,000 cycles at 10 A/g [119]. Karmur et al. fabricated a nanocomposite comprising WO_3 nanorods, reduced graphene oxide sponge (rGOsp), and MXene. WO_3 contributed its high redox properties and prevented the collapse of the MXene layers. To enhance the charge-discharge capacity, this MXene-WO_3 composite was deposited onto the porous surface of rGOsp. The study resulted in an asymmetric supercapacitor device with MXene-WO_3@rGOsp serving as the cathode electrode and porous carbon (PC) as the anode electrode. This device exhibited an impressive energy density value of 34 Wh/kg at a power density of 1450 W/kg and retained approximately 86% of its specific capacitance even after 3,000 cycles of charging and discharging (Fig. 17) [120].

Another way of improving supercapacitor performance including specific capacitance, energy density is to incorporate a conducting polymer to WO_3 structure. Das et al. produced a flexible solid-state all-solid-state asymmetric supercapacitor device utilizing nickel selenide (NiSe) as a positive electrode and WO_3/polypyrrole (WO_3@PPy) composite as a negative electrode in PVA/KOH gel as the electrolyte. The highest specific capacitance and energy density were obtained as 172 F/g and 37.3 Wh/kg at 2 A/g current density and the power density of 1249 W/kg, respectively [121]. Some research studies have focussed on the addition of conducting ions into WO_3 matrix to increase the conductivity of the metal oxide. Barik et al. worked a two-dimensional

جامعة قطر QATAR UNIVERSITY

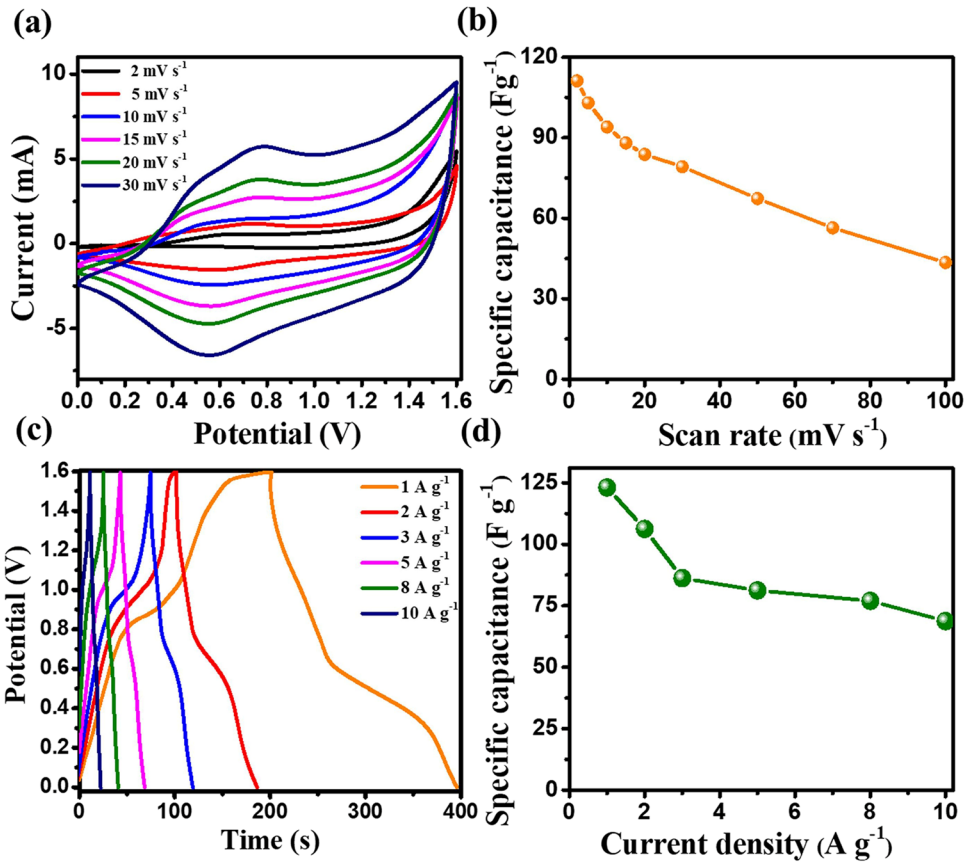


Fig. 16 (**a**) CVs at different scan rates from 2 to 30 mV/s (**b**) The specific capacitance of the WO_3 nanorod//exfoliated rGO cell was plotted against the scan rate (**c**) GCD at different current densities. (**d**) The specific capacitance of the flexible quasi-solid-state hybrid supercapacitor WO_3 nanorod//exfoliated rGO cell was measured at various current densities. Copyright 2022, Elsevier. Reprinted with permission [18]

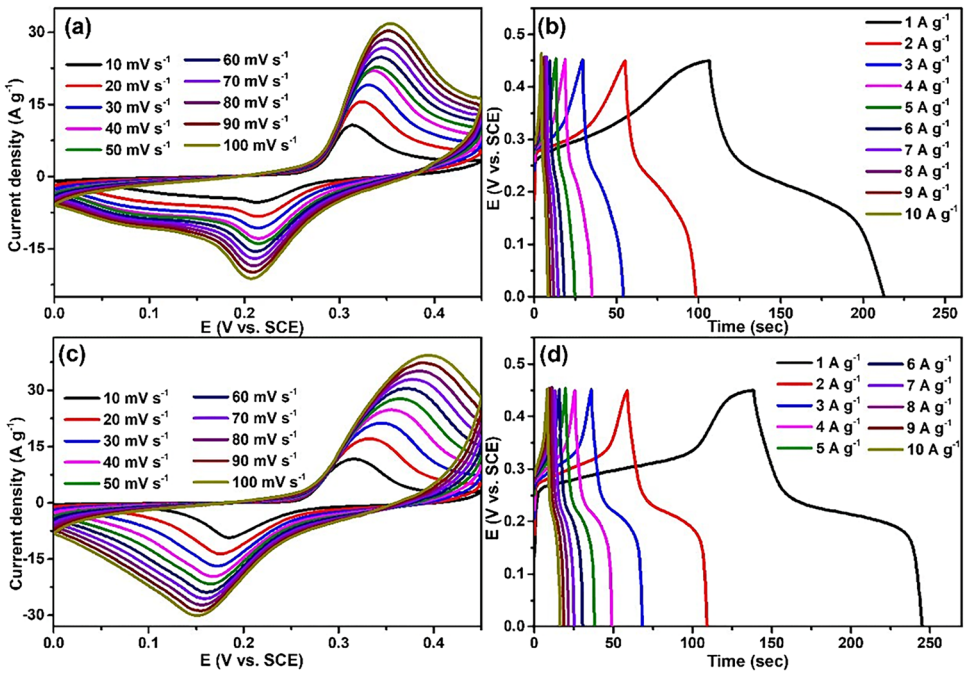


Fig. 17 CV profiles at various scan rates and GCDs at different current densities of (**a**), (**b**) MXene-WO_3 and (**c**), (**d**) MXene-WO_3@rGO_{sp} in 2 M KOH electrolyte. Copyright 2023, Elsevier. Reprinted with permission [120]

tungsten oxide/selenium (2D WO_3/Se) nanocomposite on CC current collector for flexible supercapacitor devices.

To investigate the electrochemical properties of WO_3/Se electrode based flexible ASC system, ASC system is produced using a WO_3/Se based electrode and flexible carbon cloth with PVA−H_2SO_4 gel electrolyte, as displayed in Fig. 18. CV measurements were performed within a potential window of 1.7 V without any resistance/H_2/O_2 evolution

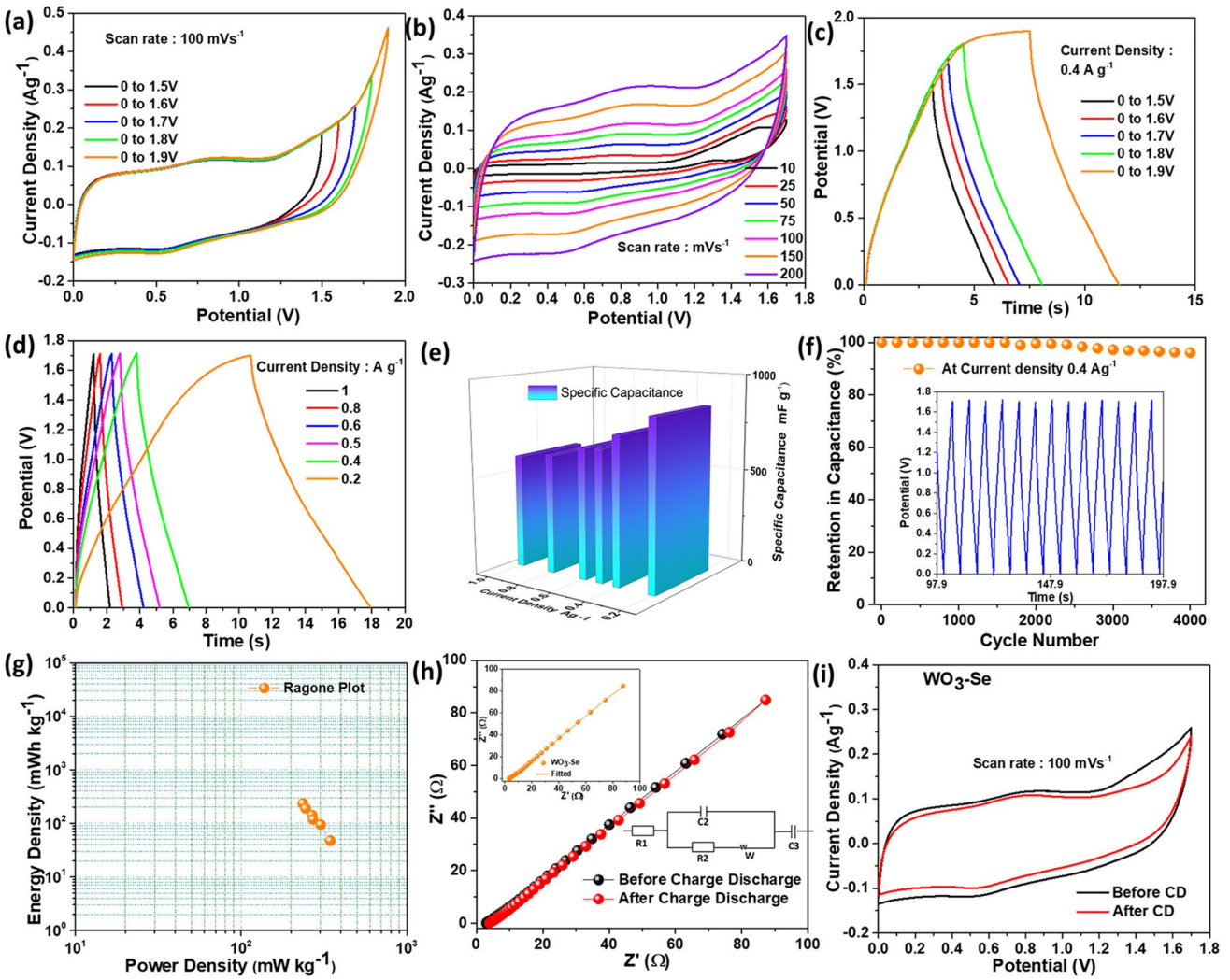


Fig. 18 CV curves for ASC system with WO_3/Se-based electrode. (**a**) Potential windows at a scan rate of 100 mV/s (**b**) at varying scan rates within potential window of 0-1.7 V (**c**) GCD curves at potential windows and (**d**) at different current densities. (**e**) Specific capacitance vs current density (**f**) Cycle stability up to 4000 cycles (**g**) Ragone plot and (**h**) EIS curve before and after cycle stability (**i**) CV curve before and after cycle stability. Copyright 2021, ACS. Reprinted with permission [122]

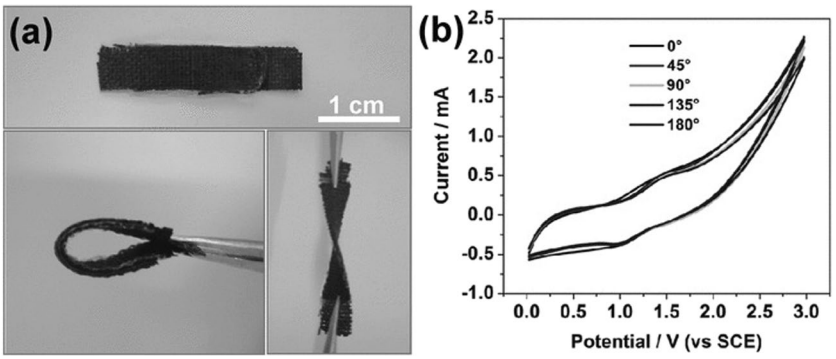


Fig. 19 (**a**) Optical images of the fabricated solid-state supercapacitor device. The lower images illustrate the exceptional flexibility of the prepared device. (**b**) CV curves of a WO_3–x@Au@MnO_2 supercapacitor captured at various angles: 0°, 45°, 90°, 135°, and 180°, within the voltage range of 0–3 V. Copyright 2012, Wiley. Reprinted with permission [125]

جامعة قطر QATAR UNIVERSITY

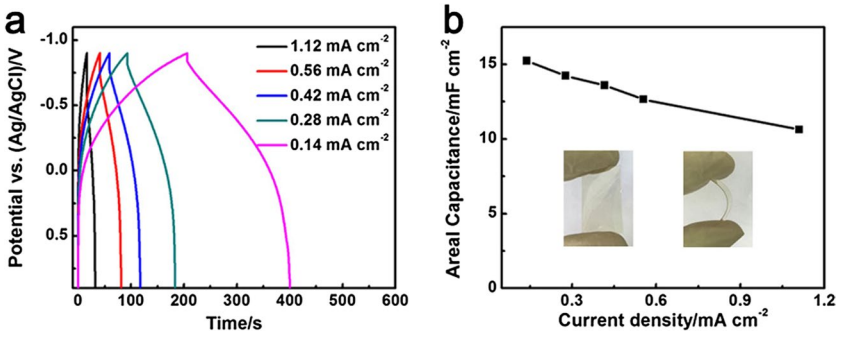


Fig. 20 (**a**) GCD profiles of the WO_3/ZnO nanocomposite electrode recorded at various current densities. (**b**) Areal capacitance of the WO_3/ZnO nanocomposite electrode plotted against the current density. The insets showcase photographs of the flexible electrode incorporating the WO_3/ZnO nanocomposites. Copyright 2017, Elsevier. Reprinted with permission [126]

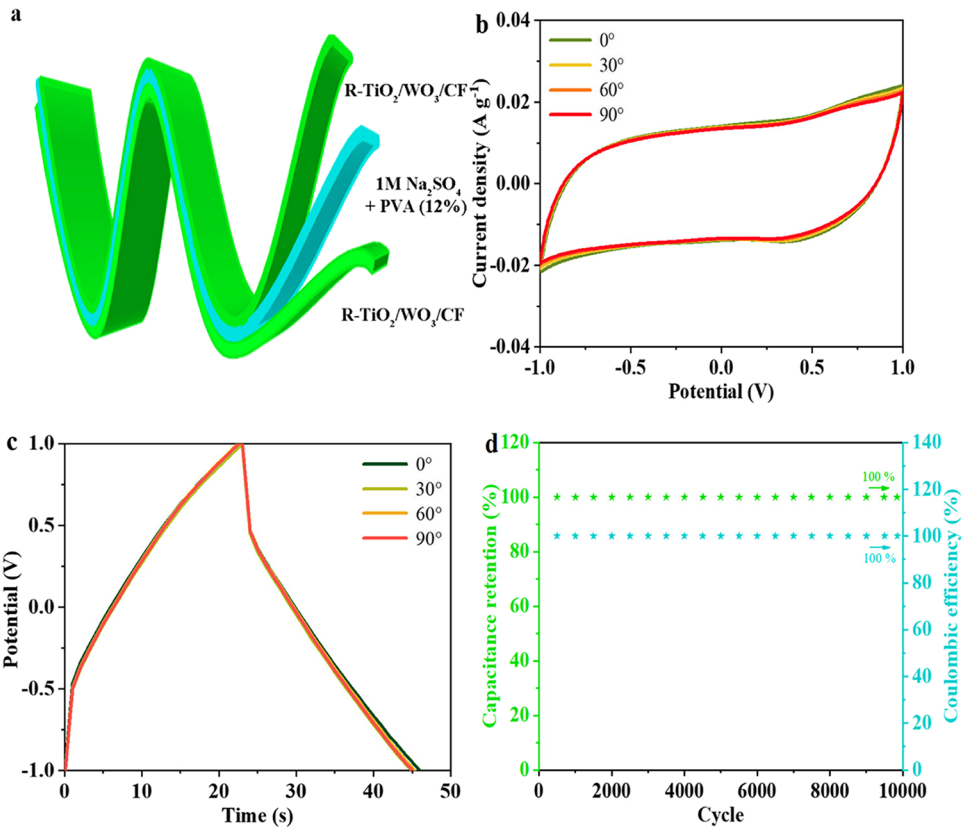


Fig. 21 (**a**) Schematic representation of the all-solid-state flexible supercapacitor, demonstrating the utilization of R-TiO_2/WO_3/CF as active electrodes and PVA + Na_2SO_4 as the gel electrolyte. (**b**) The CV curve of the device recorded at a scan rate of 20 mV/s from 0 to 90°. (**c**) The GCD curves of the device at a current density of 40 mA/g from 0 to 90°. (**d**) Long-term stability and coulombic efficiency of the device at a current density of 40 mA/g. Copyright 2023, American Chemical Society. Reprinted with permission [127]

reaction as can be displayed from Fig. 18a, b. The potential window of 0−1.7 V was optimized in this study. The diverse CV curves attained in the range of scan rates from 10 to 200 mV/s demonstrated the process of ion diffusion and charge transport enable the increased electrochemical performance. GCD curves for the ASC was shown in diverse potential windows and current densities (Fig. 18c, d). The maximum specific capacitance 858 mF/g at a potential window of 1.7 V and a current density of 0.2 A/g was attained for WO_3/Se based electrode ASC. When the current density enhances, the specific capacitance declines, as shown in Fig. 18e. The WO_3/Se electrode displayed cyclic durability up to 2,100 cycles with unchanged retention in specific capacitance and the retention was attained as 94% after 4,000 cycles (Fig. 18f). The broader potential windows allows the enhanced in energy density (47 mWh/kg) and power density (345 mW/kg) at a current density of 0.2 A/g (Fig. 18g). The Nyquist plot and equivalent circuit diagram was shown in Fig. 18h. The ASC system indicated the pure capacitive attitude of the electroactive compound. The solution resistance was calculated as 2.98 Ω. The resistance features of the ASC system was obtained before and after 4,000 charge−discharge

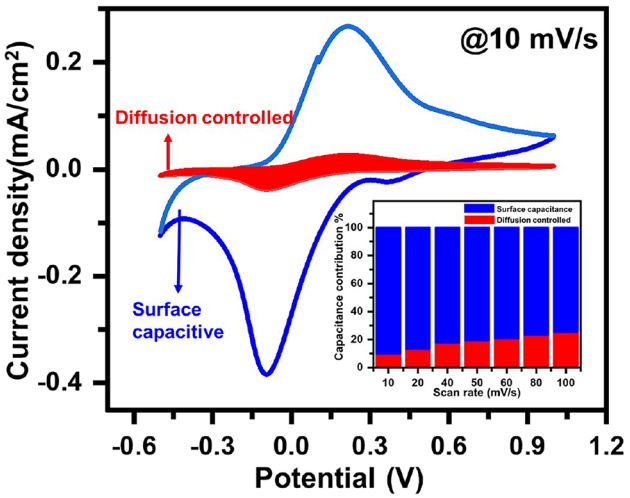


Fig. 22 Areal representation (Inset: Histogram representation) of diffusion-controlled specific capacitance and surface-controlled specific capacitance of flexible solid-state supercapacitor Co_3O_4//WO_3 device. Copyright 2023, Royal Society of Chemistry. Reprinted with permission [109]

cycles. The WO_3/Se system had almost stable performance attitude even after 4,000 cycles (Fig. 18i) [122].

An elevated mass loading of active material was used for developing the areal capacitance and energy density of the supercapacitor device. Huge quantities of active materials on the electrode alter the specific capacitance since the electrode materials in the bulk both utilized as active materials during the charge-discharge process and the surface materials can join into it [123]. It is well-known that the WO_3 electrode has specific capacitance closer to theoretical capacitance when the mass loading of WO_3 active materials is less than 1 mg/cm^2. Also, commercially used electrodes are usually necessary for high materials loading of more than 10 mg/cm^2. But, when the mass loading of WO_3 active material is generally higher than 5 mg/cm^2, it may lead to a change for a worse of its capacitive performance because of the obstacle of ion diffusion and electron transport. Thus, the limited total capacitance and energy stored in electrochemical capacitors with such a small mass loading of WO_3 considerably restrict the practical applications [124]. To improve the electrochemical performance of huge amount loaded WO_3 electrode, particularly the fast charge-discharge capability at great current density has gained a considerable challenge for supercapacitor applications [124]. In one study, the $Ti_3C_2T_x$/WO_3-based flexible electrode including ultrahigh amount loading WO_3 was fabricated onto the CC using an electrophoretic deposition technique. The experimental results show that the thick $Ti_3C_2T_x$/WO_3@CC electrode consisting of amount loading of 34.9 mg/cm^2 had a high areal 5.73 F/cm^2 (gravimetric capacitance of 164 F/g) at 5 mA/cm^2 [124]. In other study, the asymmetric supercapacitor device produced using alpha(∝)-MnO_2 and hexagonal (h)-WO_3 having enhanced theoretical capacitance and h-WO_3 as negative electrode with huge mass loading (5.8 mg/cm^2). The supercapacitor displayed an elevated areal capacitance of 377.14 mF/cm^2 at 4 mA/cm^2 [104].

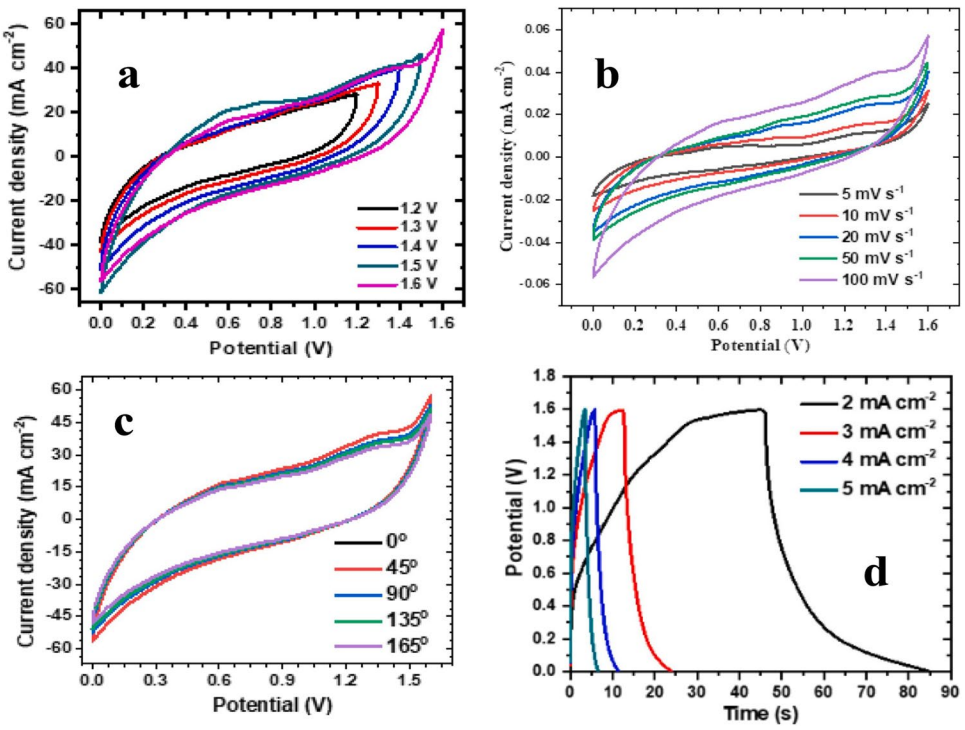


Fig. 23 Cyclic voltammograms obtained at various (**a**) potentials (**b**) scan rates and (**c**) bending angles (**d**) GCD curves at various current densities Copyright 2024, Elsevier. Reprinted with permission [128]

جامعة قطر QATAR UNIVERSITY

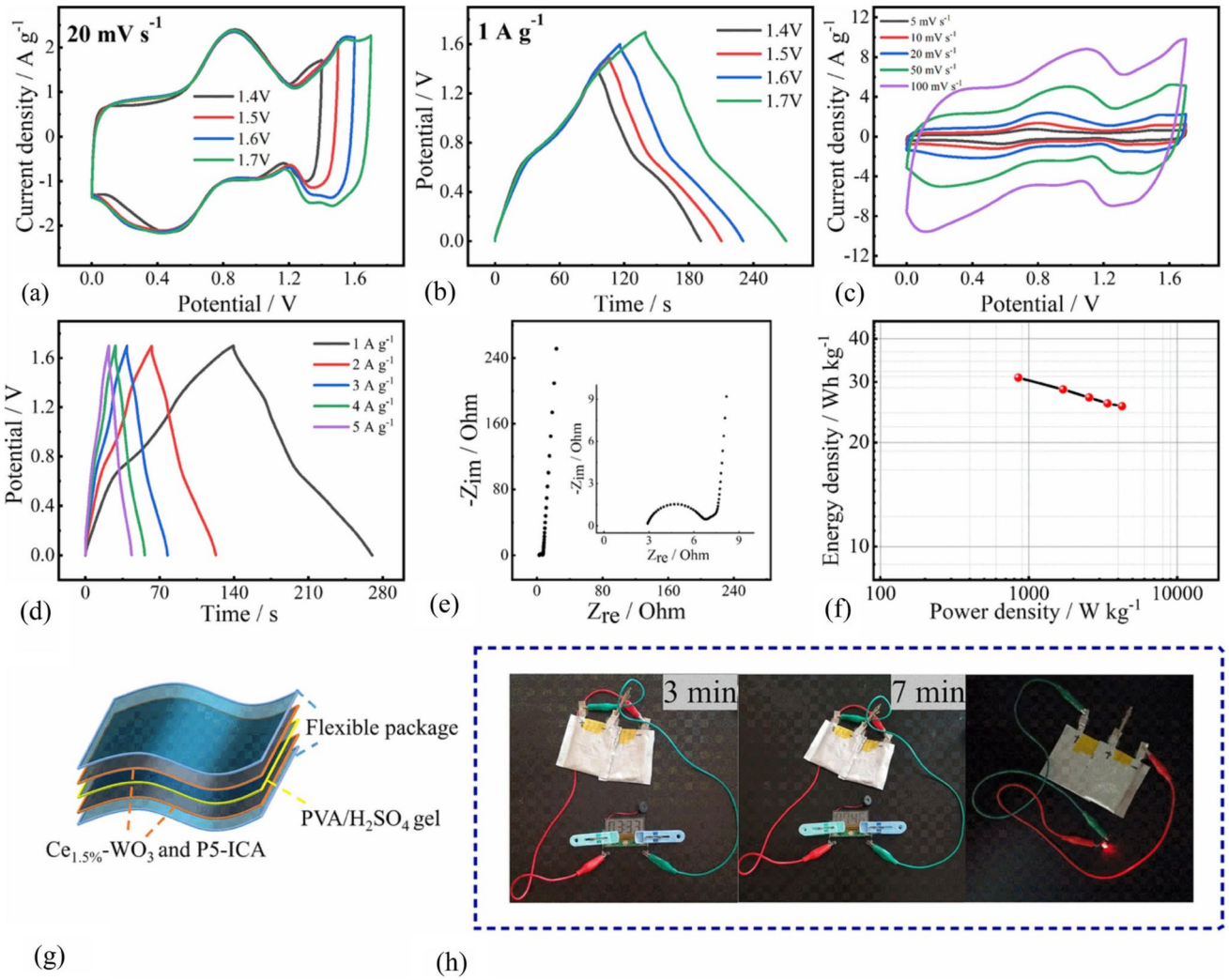


Fig. 24 Electrochemical performance of flexible all-solid-state ASC based on Ce (1.5%)-WO_3//P5-ICA using PVA/H_2SO_4 gel electrolyte: (**a**) CV profiles at various voltage windows under 20 mV/s, (**b**) GCD profiles at various voltage windows under 1 A/g, (**c**) CV curves at different scan rates, (**d**) GCD curves at different current densities, (**e**) Nyquist plot, (**f**) Ragone plot, (**g**) Schematic of a flexible ASC, (**h**) Illuminating timer and LED digital photos. Copyright 2024, Elsevier. Reprinted with permission [108]

The flexible solid-state supercapacitor device was manufactured by using two pieces of carbon fabric with WO_3–x@Au@MnO_2 hybrid structure facing each other separated via a PVA–H_3PO_4 gel electrolyte. The specific capacitance of these WO_3–x@Au@MnO_2 core–shell nanowires was obtained as 588 F/g at a scan rate of 10 mV/s and 1195 F/g at a current density of 0.75 A/g. Moreover, their results showed that au layer deposition on the WO_3 nanowire can enhance the supercapacitor performance and cyclic voltage kept almost unchanged on the different bending angles (Fig. 19) [125].

Bi et al. used the tungsten trioxide/zinc oxide (WO_3/ZnO) nanocomposites flexible electrochromic-supercapacitor applications using both a simple hydrothermal process and PLD method that displayed the enhanced capacitive performance with areal capacitance of 15.24 mF/cm^2. Characteristic galvanostatic charge/ discharge curves of WO_3/ZnO nanocomposites electrode was evaluated using diverse current densities in the voltage range between −0.9 V and 0.9 V. The electrode colour changed to dark-blue, getting to a fully charged state (−0.9 V). In opposite step, the electrode colour turns to transparent during the discharge process (0.9 V). WO_3/ZnO based electrode as a smart energy storage device can be optically follow the level of stored energy by rapid and reversible colour alteration. The areal capacitance was calculated as 15.24, 14.23, 13.59, 12.66 and 10.63 mF/cm^2 at the current densities of 0.14, 0.28, 0.42, 0.56 and 1.12 mA/cm^2, respectively, demonstrating decreased areal capacitance with enhancing current density, because of difficulties in diffusion during charge storage (Fig. 20) [126].

Huang et al. reported a study on the in situ growth of reduced hybrid metal oxides (R-TiO_2/WO_3) with oxygen vacancies on a carbon fiber (CF) substrate, aimed at developing a flexible symmetric supercapacitor. The R-TiO_2/WO_3/CF electrode as positive/negative electrodes showed a good capacitance of 102 F/g and a considerable long-term durability of about 97.64 %. The flexible symmetric supercapacitor were fabricated by sandwiching of PVA/Na_2SO_4 as a gel electrolyte between positive and negative electrodes. After applying different bending angle tests, the shape of CV and GCD curves retained any considerable difference from the initial curve. Moreover, the as-prepared device kept 100% of its initial capacitance and coulombic efficiency up to 10,000 cycles, demonstrating good mechanical stability (Fig. 21) [127].

Bansal et al. utilized flexible solid-state supercapacitor device consisting of a complementary pair of redox-active materials like WO_3 as anode and Co_3O_4 as cathode that showed improved specific capacitance, pseudocapacitive performance, mechanical durability, showing the flexible supercapacitor device that can be bend for a 180°. The highest diffusion controlled contribution was calculated as 20% at the scan rate of 100 mV/s due to unsatisfactory interaction time between electrolyte ions at the electrode-electrolyte interface (Fig. 22) [25].

Anikpa et al. investigated ASC performance of MWCNT-WO_3 composite electrode prepared using hydrothermal method. To find a suitable potential window for the process of the fabricated ASC device, a cyclic voltametric test was done by gradually widening the potential window at 50 mV/s (Fig. 23a). The cyclic voltammograms of ASC device showed a polarization phenomenon at potential voltage less than 0 V. The enhanced in the curve area was not significantly at potential voltage of more than 1.6 V. MWCNT-WO_3 as negative electrode||PANI as positive electrode based solid-state device found a suitable potential window within the range of 0 V to 1.6 V. Figure 23b shows the cyclic voltammograms of MWCNT-WO_3||PANI based solid-state device at different scan rate range from 5 mV/s to 100 mV/s. A quasi-rectangular shape without clear redox peaks was obtained [128].

The characterization of stress-strain curves is fundamental in assessing the mechanical robustness of flexible electrodes, which directly influences the operational stability and durability of flexible supercapacitors. This characterization not only elucidates the elastic and plastic deformation behaviors of the electrode materials under mechanical stress but also aids in the optimization of electrode design for enhanced mechanical resilience without compromising electrochemical performance. Studies have shown that understanding the stress-strain response enables the engineering of supercapacitors that maintain high capacitance and energy density under mechanical deformations such as bending, twisting, and stretching, thus ensuring reliable energy storage solutions for flexible and wearable electronics [129]. Moreover, this fundamental insight assists in the material selection process, guiding the development of composite electrodes that combine conductive polymers or carbonaceous materials with metal oxides like WO_3 to strike a balance between flexibility, conductivity, and capacitive behavior [130, 131].

Figure 23c displays cyclic curves at changing bending angles. CV with the bending angles from 0° to 165° was almost same demonstrating considerable mechanical flexibility of the produced device. Figure 23d shows the GCD plots of the produced ASC device at changing current densities. The specific capacitance of the ASC device was calculated as 120.7, 53.6, 34.7, and 25.6 F/g at diverse current densities [128].

Li et al. produced ASC with Ce doped WO_3 (Ce (1.5%) -WO_3) nanowire as anode, poly (indole-5-carboxylic acid) (P5-ICA) as cathode, PVA-H_2SO_4 gel as the electrolyte. Figure 24a shows the alteration of ASC under diverse voltage windows of 0–1.7 V at 20 mV/s, demonstrating that the ASC can use the operating potential of 1.7 V. Two redox peaks are clear demonstrated that the charge storage mechanism is practically faraday. As seen in Fig. 24b, diverse voltage windows were calculated at 1 A/g. The best symmetrical GCD curve was obtained at a high voltage of 1.7 V. The pseudo-capacitance characteristic of the electrode material was shown from the GCD curve In Fig. 24c and d. Nyquist plot showed a low internal resistance and ideal capacitance property (Fig. 24e). The power density of ASC possesses an energy density of 30.9 Wh/kg and a power density of up to 850 W/kg (Fig. 24f). Schematic of a flexible ASC was shown in Fig. 24g. Two all solid-state soft-packaged ASCs in series

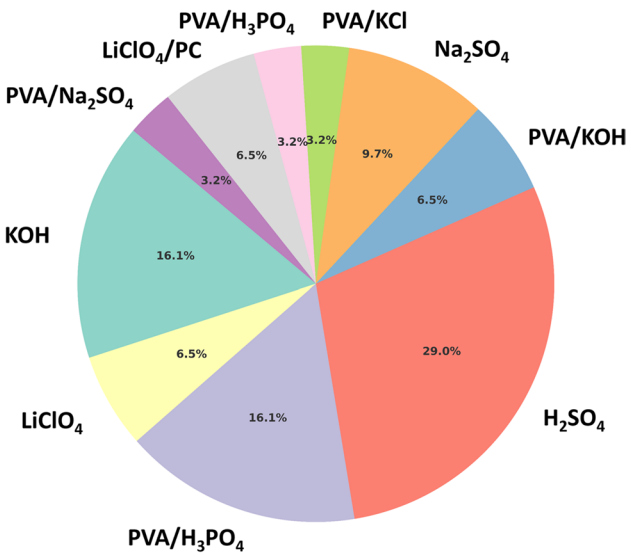


Fig. 25 Graphical representation of flexible WO_3-based thin films for supercapacitors using a variety of electrolytes, as detailed in Table 2

جامعة قطر QATAR UNIVERSITY

Table 2 Comparison of capacitance for flexible supercapacitor applications using WO_3 based electrodes

Materials	Fabrication Method	Electrolyte	Current Density	Specific capacitance	Potential Interval (V)	Cyclic stability (cycles) and Retention (%)	Ref.
WO_3	Hydrothermal	6 M KOH	-	64 F/g	0–0.8	-	[117]
WO_3	Magnetron sputtering	1 M $LiClO_4$	1 mA/cm^2	9.76 mF/cm^2	(−0.6)–0	5,000 cycles and 69.53%	[116]
WO_3 nanorods	Hydrothermal	PVA/H_2SO_4 gel	1 A/g	123 F/g	0–1.6	2,000 cycles and 92%	[18]
WO_3 nanoflowers	Electrodeposition	1 M H_2SO_4	6 mA/cm^2	684.5 mF/cm^2	(−0.5)–0	5,000 cycle and 85%	[23]
WO_3	PLD	PVA/KOH gel	3.2 A/cm^3	141.9 F/cm^3	0–1.6	27,000 cycles and 91%	[103]
WO_3 nanotube	Hydrothermal	0.5 M H_2SO_4	3 mA/cm^2	2575 mF/cm^2	0– (−0.7)	6,000 cycles and 85.1%	[20]
WO_3@ACC	Simple alcohol-thermal	Na_2SO_4	5 mA/cm^2	659 mF/cm^2	(−1.0)– (−0.3)	10,000 cycles and ~100%	[22]
2D WO_3/Se	Hydrothermal	PVA/H_2SO_4 gel	0.2 A/g	858 mF/g	0–1.7	4,000 cycles and 94%	[122]
rGO/WO_3	Electrochemical deposition	H_2SO_4	8 A/g	25.8 mF/cm^2	(−0.5)–0.5	-	[105]
WO_3@$W_{18}O_{49}$-CNFs	Electrospinning & high-temperature roasting	4 M KOH	0.5 A/g	333.92 F/g	(−0.85)–0.05	5,000 cycles and 98.2%	[113]
LC-WO_3	In-situ growing	PVA/H_2SO_4 gel	2 mA/cm^2	1693 mF/cm^2	0–1.7	10,000 cycles and 92%	[21]
WO_3 fiber	Hydrothermal	0.5 M H_2SO_4	2 A/g	539.42 F/g	(−0.65)–0	6,000 cycles and 79.1%	[68]
MWCNTs-WO_3-graphite sheet	Chemical dealloying	1.0 M H_2SO_4	1.5 A/g	103 F/g	0–1.5	2,000 cycles and 96%	[118]
WO_3	Hydrothermal	1 M Na_2SO_4	2 mA/cm^2	480 F/g	(−0.6)– 0	2,000 cycles and 86%	[79]
h-WO_3	Hydrothermal	1 M Na_2SO_4	4 mA/cm^2	377.14 mF/cm^2	(−0.7)– 0	-	[123]
MXene-WO_3@rGOsp	Dispersion	2 M KOH	1 A/g	505.7 F/g	0–0.45	3,000 cycles and 86%	[120]
$Ti_3C_2T_x$/WO_{3-x}	Solvothermal	3M H_2SO_4	-	442.0 F/g	(−1)– (−0.3)	10,000 cycles and 90.21%	[119]
$Ti_3C_2T_x$/WO_3@CC	Electrochemical deposition	1 M H_2SO_4	5 mA/cm^2	164 F/g	(−0.35)–0.2	6,000 cycles and 86.2%	[124]
NiSe//WO_3@PPy	Hydrothermal//in situ oxidative polymerization	PVA/KOH gel	2 A/g	172 F/g	0–1.25	5,000 cycles and 91%	[121]
WO_3-CeO_2 nanowire	Hydrothermal	1 M H_2SO_4	2 mA/cm^2	1310 mF /cm^2	(−0.6)–0	3,000 cycle and 92.4%	[24]
Co_3O_4//WO_3	Electrodeposition	PVA/KCl gel	0.1 mA/cm^2	66.5 mF/cm^2	(−0.5)– 1	500 cycles and 80%	[25]
WO_3–x@Au@MnO_2 core–shell nanowires	Physical evaporation deposition	PVA/H_3PO_4 gel	0.75 A/ g	1195 F/g	0–0.8	5,000 cycles and 110%	[125]
WO_3/ZnO	PLD	1 M $LiClO_4$/PC	0.14 mA/cm^2	15.24 mF/cm^2	(−0.9)–0.9	-	[126]
R-TiO_2/WO_3	Hydrothermal	PVA/Na_2SO_4 gel	1000 mA/g	102 F/g	(−1)–1	10,000 cycles and 97.64%	[127]
WO_3/SiO_2/WO_3	RF Magnetron sputtering	1 M $LiClO_4$/PC	0.06 mA/cm^2	10.13 mF/cm^2	(−1.2)–0.4	500 cycles	[132]
MWCNT-WO_3	Hydrothermal	PVA/H_2SO_4 gel	2 mA/cm^2	120.7 F/g	0–1.6	5,000 cycles and 80%	[128]
Ce (1.5%)-WO_3	solvothermal	PVA/H_2SO_4	4 A/g	493 F/g	0–1.7	5,000 cycles and 90.4%	[108]
($NiMoO_4$)/WO_3	Drop casting	3 M KOH	1 A/g	429.46 F/g	0–0.5	10,000 cycles and 89.9%	[137]

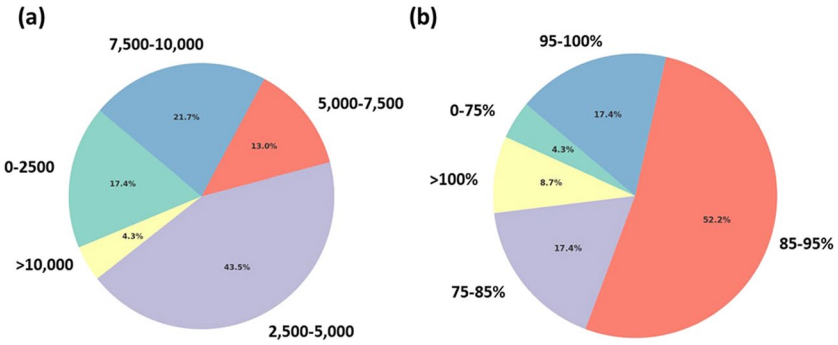


Fig. 26 Graphical representation of flexible WO_3-based thin film electrodes, focusing on (**a**) cyclic stability and (**b**) capacity retention, as outlined in Table 2

successfully brightened LEDs and time (Fig. 24h). The specific capacitance of Ce (1.5%)-WO_3 was calculated as 493 F/g at 4 A/g and remains 90.4 % after 5,000 cycles [108].

In order to enhance the capacitive performance of WO_3 nanomaterials, some scientific research focused on the method of WO_3 nanomaterials immediately growing on a conductive substrate [102]. For instance, Qui et al. produced the WO_3 nanoflowers onto Ti foil using electrodeposition method. The produced electrode showed an areal specific capacitance of 684.5 mF/cm^2. The Nyquist plot from EIS result showed that the produced electrode had significant conductivity with a low equivalent series impedance of only 173 mΩ [23]. Though the WO_3 nanomaterials immediately depositing on the conductive substrate can considerably decrease the contact resistance, the low intrinsic conductivity of WO_3 itself still allow to the obstacle of electron transfer in the bulk phase, thus have hard in attaining the required capacitance value [24]. He et al. introduced a novel approach to significantly enhance the electron transport within the electrode material. Their method involved the fabrication of WO_3-CeO_2 hybrid nanowires using a hydrothermal technique. These nanowires were carefully integrated onto the surface of a rough poly(3,4-ethylene dioxythiophene) (PEDOT) electrode that was deposited on a glassy carbon (GC) substrate. To further optimize the conductivity, a conductive layer of poly(3,4-ethylene dioxythiophene): polystyrene sulfonate (PEDOT: PSS) was applied as the outermost layer. This unique combination of materials and their precise arrangement resulted in a robust and efficient electron transport pathway throughout the electrode material, thereby improving the overall performance of the supercapacitor. The considerable contributions of this design as follows was shown: (1) Due to structural and electrical features of PEDOT thin layer including porous structure, high conductivity, it can be enhanced the specific area of the electrode, moreover electrostatic interaction between W cation from WO_3-based nanowires and SO_3^- anion from PEDOT:PSS can be occurred (2) PEDOT:PSS solution with elevated conductivity and interface suitability can leak into the porous layer of WO_3-based nanowires to behave as a conductive linkage, in addition to, the PEDOT:PSS layer can effectually prevent from the dissolution and shedding of WO_3-based nanowires. Electrochemical results showed that as-fabricated PEDOT:PSS/WO_3/PEDOT/GC and PEDOT:PSS/WO_3-CeO_2/PEDOT/GC electrodes had an elevated areal capacitance of 1139.6 and 1310 mF/cm^2 at 2 mA/cm^2, respectively [24].

Muslu et al. utilized WO_3/SiO_2/WO_3 thin film onto on a flexible Cu substrate using RF magnetron sputtering method for supercapacitor applications. The WO_3/SiO_2/WO_3 thin film thin film showed high specific capacitances of 10.13, 8.95, 8.28, 4.34, and 5.66 mF/cm^2 at current densities of 0.06, 0.2, 0.4, 0.8, and 1.2 mA/cm^2, respectively due to the synergistic effect of Li^+ diffusion [132].

In optimizing WO_3-based flexible supercapacitors, the choice of electrolyte is paramount, significantly influencing ionic conductivity, mechanical flexibility, and electrochemical stability. Aqueous electrolytes, praised for their conductivity and eco-friendliness, are limited by a lower electrochemical window, potentially restricting energy density [133]. Organic electrolytes extend this window but come with environmental and safety concerns [134]. Ionic liquids offer a balanced solution with wide electrochemical windows and high thermal stability, albeit at a higher cost and viscosity [135]. Gel polymer electrolytes emerge as a promising alternative, blending polymer mechanical integrity with liquid electrolyte conductivity, enhancing both the device's flexibility and safety [136].

The integration of WO_3 nanocomposites into polymer electrolytes presents a significant advancement, combining WO_3's high capacitance with the polymer's durability to boost supercapacitor performance [131]. Figure 25 illustrates that recent studies have employed various electrolytes in WO_3-based thin films for supercapacitors.

Table 2 presents data on the capacitance performance of flexible WO_3-based thin film electrodes, highlighting their application in supercapacitors with the electrolytes used. Analysis of Table 2, which details WO_3-based flexible thin film electrodes, reveals a substantial variability in cyclic stability, with a range between 2,500 and 5,000 cycles (Fig. 26a). Moreover, these electrodes showcase superior capacity retention, achieving 85 % to 95 % of their original capacity (Fig. 26b). This high performance is attributed to the distinct flexibility and functional attributes of WO_3, making them exceptionally apt for supercapacitor applications.

جامعة قطر QATAR UNIVERSITY

4 Conclusion and future scope

The increasing interest in flexible supercapacitors, driven by their potential applications in storage solutions, wearable and portable electronic devices, the Internet of Things (IoT), and transportation, has sparked significant market expansion. Flexible supercapacitors, known for their adaptability in various applications, represent a cutting-edge technology that combines high energy density and long cycle life with exceptional electrical conductivity.

In 2023, the global market for flexible supercapacitors was estimated to be approximately USD 322 million. Forecasts predict a Compound Annual Growth Rate (CAGR) of 3.5% through to the year 2029, highlighting the growing investment and development in this sector (https://reports.valuates.com/market-reports/QYRE-Auto-27X9862/global-flexible-super-capacitor). The focus on developing suitable flexible technologies for the future centers on leveraging thin film-based electrodes, which are pivotal for enhancing the performance and efficiency of supercapacitor technology [7].

In this point, WO_3 stands out among potential electrode materials due to its stability, affordability, eco-friendly properties, and impressive theoretical capacity. In this review, historical development, charge discharge mechanisms, analyses to evaluate supercapacitor performance and techniques for fabricating WO_3-based flexible films are overseen.

Researchers have been experimenting with various approaches to enhance the efficiency of WO_3-based flexible supercapacitors. These methods include utilizing nanostructured WO_3 materials and combining them with diverse advanced materials in composite forms. In addition, these innovative techniques and approaches have shown promising results, significantly enhancing the performance of flexible supercapacitors based on WO_3. However, there is required for further efforts to facilitate large-scale commercial applications in flexible energy storage, wearable devices, and portable electronics.

In future, it seems that WO_3-based thin film electrodes for supercapacitors will lie in improving energy density, cycling stability, and flexible applications. Proceeding research will focus on developing environmentally friendly production methods, ensuring scalability, and integrating these electrodes with energy harvesting technologies for sustainable energy solutions. Additionally, deep into the subject through theoretical modelling and simulation will provide invaluable insights. Such approaches will not only influence the tendency of supercapacitor development but also provide the precise design of energy storage systems and their components, ensuring they are highly efficient and qualified for superior performance [138, 139].

This section outlooks the innovative research pathways and technological trends that are expected to shape the future landscape of supercapacitor development, particularly focusing on WO_3-based thin films item by item:

1. Nanomaterials and hybrid composites: The integration of nanoscale materials with WO_3 offers a promising strategy to enhance the electrochemical performance of supercapacitors. Future research will like probably focus on the synthesis of hybrid composites combining WO_3 with carbon nanotubes, graphene, conductive polymers, MXene or other transition metal oxides such MoO_3, MnO_2, and so on. These composites aim to exploit the unique properties of each component, such as the high conductivity of graphene and the pseudocapacitance of conductive polymers, to achieve superior energy storage capabilities. Tailoring the interface between WO_3 and these nanomaterials will be crucial for optimizing charge transfer and mechanical flexibility.
2. Advanced fabrication techniques: Emerging fabrication techniques such as atomic layer deposition, electrospinning, and laser-induced synthesis present new avenues for producing WO_3 thin films with precise control over thickness, porosity, and morphology. These methods enable the creation of highly uniform and conformal coatings, which are essential for maximizing surface area and enhancing the interaction between electrode materials and electrolytes. The development of scalable and environmentally friendly fabrication processes will be a key area of focus, aiming to reduce production costs and improve the sustainability of supercapacitor manufacturing.
3. Electrolyte innovation: The interaction between WO_3 electrodes and electrolytes plays a pivotal role in the performance of supercapacitors. Research into novel electrolytes, including ionic liquids and solid-state electrolytes, offers the potential to significantly increase energy density and widen the operational temperature range. The compatibility of these electrolytes with WO_3-based thin films and their impact on ion transport dynamics and interfacial stability will be critical areas of investigation.
4. System integration and real-world applications: Looking forward, the integration of WO_3-based supercapacitors into real-world applications will require innovative approaches to device engineering and system architecture. Wearable electronics, flexible displays, and smart textiles represent exciting opportunities for incorporating energy storage solutions that are thin, lightweight, and flexible. Collaborations between material scientists, engineers, and industry partners will be vital in translating laboratory-scale advancements into commercially viable products.

5. Theoretical and computational insights: Advancements in theoretical models and computational simulations will continue to provide valuable insights into the fundamental mechanisms governing the performance of WO_3-based supercapacitors. High-throughput screening of materials, molecular dynamics simulations, and density functional theory calculations can help identify optimal material compositions and structures, guiding experimental efforts and accelerating the discovery of next-generation electrode materials.

Author contributions EM contributed to the corresponding author, researching, data curation, methodology, writing original draft preparation, reviewing and editing; EE contributed to researching, data curation, methodology, writing original draft preparation, reviewing and editing; AUO contributed to the corresponding author, researching, data curation, methodology, writing original draft preparation, reviewing, and editing.

Funding The authors declare that no funds, grants, or other support were received during the preparation of this manuscript.

Data availability The authors declare that all data supporting the findings of this study are available within the article.

Declarations

Conflict of interest The authors have no relevant financial or non-financial interests to disclose.

Open Access This article is licensed under a Creative Commons Attribution 4.0 International License, which permits use, sharing, adaptation, distribution and reproduction in any medium or format, as long as you give appropriate credit to the original author(s) and the source, provide a link to the Creative Commons licence, and indicate if changes were made. The images or other third party material in this article are included in the article's Creative Commons licence, unless indicated otherwise in a credit line to the material. If material is not included in the article's Creative Commons licence and your intended use is not permitted by statutory regulation or exceeds the permitted use, you will need to obtain permission directly from the copyright holder. To view a copy of this licence, visit http://creativecommons.org/licenses/by/4.0/.

References

1. A. Khorate, A.V. Kadam, An overview of patents and recent development in flexible supercapacitors. J. Energy Storage **52**, 104887 (2022). https://doi.org/10.1016/J.EST.2022.104887
2. A.G. Olabi, Q. Abbas, A. Al Makky, M.A. Abdelkareem, Supercapacitors as next generation energy storage devices: properties and applications. Energy **248**, 123617 (2022). https://doi.org/10.1016/J.ENERGY.2022.123617
3. S.M. Benoy, M. Pandey, D. Bhattacharjya, B.K. Saikia, Recent trends in supercapacitor-battery hybrid energy storage devices based on carbon materials. J. Energy Storage **52**, 104938 (2022). https://doi.org/10.1016/J.EST.2022.104938
4. P.C. Okonkwo, E. Collins, E. Okonkwo, Application of biopolymer composites in super capacitor. Biopolymer Composites Electron, 487–503 (2017). https://doi.org/10.1016/B978-0-12-809261-3.00018-8
5. J. Jiang, Y. Li, J. Liu, X. Huang, C. Yuan, X.W. Lou, Recent advances in metal oxide-based electrode architecture design for electrochemical energy storage. Adv. Mater. **24** (2012). https://doi.org/10.1002/adma.201202146
6. Z. Qi, S. Huang, A. Younis, D. Chu, S. Li, in *Supercapacitor Design and Applications*. Nanostructured Metal Oxides-Based Electrode in Supercapacitor Applications (2016). https://doi.org/10.5772/65155
7. Lichchhavi, A. Kanwade, P.M. Shirage, A review on synergy of transition metal oxide nanostructured materials: Effective and coherent choice for supercapacitor electrodes. J Energy Storage **55**, 105692 (2022). https://doi.org/10.1016/J.EST.2022.105692
8. Q.A. Sial, M.S. Javed, Y.J. Lee, L.T. Duy, H. Seo, Flexible and transparent graphene-based supercapacitors decorated with nanohybrid of tungsten oxide nanoflakes and nitrogen-doped-graphene quantum dots. Ceram. Int. **46**, 23145–23154 (2020). https://doi.org/10.1016/J.CERAMINT.2020.06.094
9. Y. Wang, X. Wu, Y. Han, T. Li, Flexible supercapacitor: Overview and outlooks. J Energy Storage **42**, 103053 (2021). https://doi.org/10.1016/J.EST.2021.103053
10. M.A.A. Mohd Abdah, N.H.N. Azman, S. Kulandaivalu, Y. Sulaiman, Review of the use of transition-metal-oxide and conducting polymer-based fibres for high-performance supercapacitors. Mater. Des. **186** (2020). https://doi.org/10.1016/j.matdes.2019.108199
11. S. Adhikari, M. Murmu, D.H. Kim, Core-shell Engineered WO3 Architectures: recent advances from design to applications. Small **18** (2022). https://doi.org/10.1002/smll.202202654
12. B. Rodríguez, J. Dolado, J. López-Sánchez, P. Hidalgo, B. Méndez, Room temperature polymorphism in WO3 produced by resistive heating of W wires. Nanomaterials **13** (2023). https://doi.org/10.3390/nano13050884
13. D. Hafedh, K. Kaouther, B.C.L. Ahmed, Multi-property improvement of TiO2-WO3 mixed oxide films deposited on 316L stainless steel by electrophoretic method. Surf. Coat. Technol. **326**, 45–52 (2017). https://doi.org/10.1016/J.SURFCOAT.2017.07.041
14. Y. Xiao, M. Jiang, M. Cao, Developing WO3 as high-performance anode material for lithium-ion batteries. Mater. Lett. **285** (2021). https://doi.org/10.1016/j.matlet.2020.129129
15. P. Bhojane, P.M. Shirage, Facile preparation of hexagonal WO3 nanopillars and its reduced graphene oxide nanocomposites for high-performance supercapacitor. J. Energy Storage **55**, 105649 (2022). https://doi.org/10.1016/J.EST.2022.105649
16. X. Dong, Y. Liu, S. Zhu, Y. Ou, X. Zhang, W. Lan, H. Guo, C. Zhang, Z. Liu, S. Ju, Y. Miao, Y. Zhang, H. Li, Architecting hierarchical WO3 agglomerates assembled with straight and parallel aligned nanoribbons enabling high capacity and robust stability of lithium storage. Front Chem **9** (2022). https://doi.org/10.3389/fchem.2021.834418
17. H. Huang, X. Ju, H. Li, B. Qu, T. Wang, Construction of complex WO3-SnO2 hollow nanospheres as a high-performance anode for lithium-ion batteries. J. Alloys Compd. **744**, 375–380 (2018). https://doi.org/10.1016/J.JALLCOM.2018.02.090
18. S.P. Gupta, M.A. More, D.J. Late, P.S. Walke, Highly ordered nano-tunnel structure of hydrated tungsten oxide nanorods for superior flexible quasi-solid-state hybrid supercapacitor. Appl. Surf. Sci. **545**, 149044 (2021). https://doi.org/10.1016/J.APSUSC.2021.149044
19. X. Liu, S. Chen, Z. Xiong, K. Li, Y. Zhang, Tungsten oxide-based nanomaterials for supercapacitors: Mechanism, fabrication, characterization, multifunctionality, and electrochemical performance. Prog. Mater. Sci. **130**, 100978 (2022). https://doi.org/10.1016/J.PMATSCI.2022.100978

20. X. Wu, S. Yao, Flexible electrode materials based on WO3 nanotube bundles for high performance energy storage devices. Nano Energy **42**, 143–150 (2017). https://doi.org/10.1016/J.NANOEN.2017.10.058
21. J. Chen, H. Wang, J. Deng, C. Xu, Y. Wang, Low-crystalline tungsten trioxide anode with superior electrochemical performance for flexible solid-state asymmetry supercapacitor. J. Mater. Chem. A Mater. **6** (2018). https://doi.org/10.1039/c8ta01323c
22. Z. Yin, Y. Bu, J. Ren, S. Chen, D. Zhao, Y. Zou, S. Shen, D. Yang, Triggering superior sodium ion adsorption on (2 0 0) facet of mesoporous WO3 nanosheet arrays for enhanced supercapacitance. Chem. Eng. J. **345** (2018). https://doi.org/10.1016/j.cej.2018.03.100
23. M. Qiu, P. Sun, L. Shen, K. Wang, S. Song, X. Yu, S. Tan, C. Zhao, W. Mai, WO3 nanoflowers with excellent pseudo-capacitive performance and the capacitance contribution analysis. J. Mater. Chem. A Mater. **4** (2016). https://doi.org/10.1039/c6ta00237d
24. Y. He, A. Liang, D. Zhu, M. Hu, L. Xu, S. Chao, W. Zhou, Y. Wu, J. Xu, F. Zhao, Organic-inorganic hybrid electrode engineering for high-performance asymmetric supercapacitor based on WO3-CeO2 nanowires with oxygen vacancies. Appl. Surf. Sci. **573** (2022). https://doi.org/10.1016/j.apsusc.2021.151624
25. L. Bansal, S. Kandpal, T. Ghosh, C. Rani, B. Sahu, D.K. Rath, R. Kumar, Supercapacitive all-inorganic nano metal-oxides' Complex: a 180o Super-Bendable asymmetric energy storage device. J. Mater. Chem. C Mater. (2023). https://doi.org/10.1039/D3TC02677A
26. D. Malavekar, S. Pujari, S. Jang, S. Bachankar, J.H. Kim, Recent development on transition metal oxides-based core–shell structures for boosted energy density supercapacitors. Small (2024). https://doi.org/10.1002/smll.202312179
27. T.G. Novak, J. Kim, P.A. DeSario, S. Jeon, Synthesis and applications of WO3nanosheets: The importance of phase, stoichiometry, and aspect ratio. Nanoscale Adv. **3** (2021). https://doi.org/10.1039/d1na00384d
28. V. Lokhande, A. Lokhande, G. Namkoong, J.H. Kim, T. Ji, Charge storage in WO 3 polymorphs and their application as supercapacitor electrode material. Results Phys. **12**, 2012–2020 (2019). https://doi.org/10.1016/j.rinp.2019.02.012
29. Y. Shi, M. Sun, Y. Zhang, J. Cui, Y. Wang, X. Shu, Y. Qin, H.H. Tan, J. Liu, Y. Wu, Structure modulated amorphous/crystalline WO3 nanoporous arrays with superior electrochromic energy storage performance. Sol. Energy Mater. Sol. Cells **212**, 110579 (2020). https://doi.org/10.1016/J.SOLMAT.2020.110579
30. S. Shalini, T.B. Naveen, D. Durgalakshmi, S. Balakumar, R.A. Rakkesh, Progress in flexible supercapacitors for wearable electronics using graphene-based organic frameworks. J. Energy Storage **86** (2024). https://doi.org/10.1016/j.est.2024.111260
31. J. Hu, M. Dong, Recent advances in two-dimensional nanomaterials for sustainable wearable electronic devices. J. Nanobiotechnology **22** (2024). https://doi.org/10.1186/s12951-023-02274-7
32. J. Li, H. Yu, Y. Lv, Z. Cai, Y. Shen, L. Ruhlmann, L. Gan, M. Liu, Electrode materials for electrochromic supercapacitors. Nanotechnology **35**, 152001 (2024). https://doi.org/10.1088/1361-6528/ad18e2
33. V.R. Buch, A.K. Chawla, S.K. Rawal, Review on electrochromic property for WO3 thin films using different deposition techniques. Mater. Today Proc. (2016). https://doi.org/10.1016/j.matpr.2016.04.025
34. M. Bouroushian, D. Karoussos, T. Kosanovic, B.E. Conway, *Electrochemical supercapacitors: scientific fundamentals and technological applications* (Kluwer Academic/Plenum Publisher, New York, 1999, Solid State Ion 177, 2006)
35. M. Yu, X. Feng, Thin-film electrode-based supercapacitors. Joule **3**, 338–360 (2019). https://doi.org/10.1016/J.JOULE.2018.12.012
36. W.J. Li, Z.W. Fu, Nanostructured WO3 thin film as a new anode material for lithium-ion batteries. Appl. Surf. Sci. **256**, 2447–2452 (2010). https://doi.org/10.1016/J.APSUSC.2009.10.085
37. C. Cai, D. Guan, Y. Wang, Solution processing of V2O5-WO3 composite films for enhanced Li-ion intercalation properties. J. Alloys Compd. **509** (2011). https://doi.org/10.1016/j.jallcom.2010.09.129
38. P.A. Shinde, S.C. Jun, Review on recent progress in the development of tungsten oxide based electrodes for electrochemical energy storage. ChemSusChem **13** (2020). https://doi.org/10.1002/cssc.201902071
39. B.X. Zou, Y. Wang, F. Huang, Synthesis and pseudocapacitve properties of tungsten oxide nanorods. Adv. Mater. Res. (2014). https://doi.org/10.4028/www.scientific.net/AMR.968.72
40. B. Öztetïk, S. Pat, Ş. Korkmaz, Investigation on the optical and electrochromic characteristics of thin films of WO3 doped with graphene and MXene (Ti2AlC). Ceram. Int. **50**, 13113–13124 (2024). https://doi.org/10.1016/j.ceramint.2024.01.221
41. A. Ray, A. Roy, S. Saha, S. Das, Studies on electrochemical properties of Ni-Mn-oxides for advance energy storage application. ECS Meeting Abstracts MA2018-01 (2018). https://doi.org/10.1149/ma2018-01/1/142
42. B.G. Pollet, I. Staffell, J.L. Shang, V. Molkov, in *Alternative Fuels and Advanced Vehicle Technologies for Improved Environmental Performance: Towards Zero Carbon Transportation*. Fuel-cell (hydrogen) electric hybrid vehicles (2014), pp. 685–735. https://doi.org/10.1533/9780857097422.3.685
43. A. Bello, R.A. Ahmed, R.K. Koech, K. Orisekeh, D.M. Sanni, M. Kigozi, V. Anye, O.K. Oyewole, W.O. Soboyejo, in *Reference Module in Materials Science and Materials Engineering*. The Mechanical Properties of Batteries and Supercapacitors (2023), pp. 308–348. https://doi.org/10.1016/B978-0-12-822944-6.00050-5
44. J.M. Lim, Y.S. Jang, H. Van, T. Nguyen, J.S. Kim, Y. Yoon, B.J. Park, D.H. Seo, K.K. Lee, Z. Han, K. Ostrikov, S.G. Doo, Advances in high-voltage supercapacitors for energy storage systems: materials and electrolyte tailoring to implementation. Nanoscale Adv. **5** (2023). https://doi.org/10.1039/d2na00863g
45. P. Forouzandeh, V. Kumaravel, S.C. Pillai, Electrode materials for supercapacitors: a review of recent advances. Catalysts **10** (2020). https://doi.org/10.3390/catal10090969
46. X. Zhu, Recent advances of transition metal oxides and chalcogenides in pseudo-capacitors and hybrid capacitors: a review of structures, synthetic strategies, and mechanism studies. J. Energy Storage **49**, 104148 (2022). https://doi.org/10.1016/J.EST.2022.104148
47. S. Rajagopal, R. Pulapparambil Vallikkattil, M. Mohamed Ibrahim, D.G. Velev, Electrode materials for supercapacitors in hybrid electric vehicles: challenges and current progress. Condens. Matter. 7 (2022). https://doi.org/10.3390/condmat7010006
48. N. Kumar, S. Bin Kim, S.Y. Lee, S.J. Park, Recent advanced supercapacitor: a review of storage mechanisms, electrode materials, modification, and perspectives. Nanomaterials **12** (2022). https://doi.org/10.3390/nano12203708
49. D. Gao, Z. Luo, C. Liu, S. Fan, A survey of hybrid energy devices based on supercapacitors. Green Energy Environ. (2022). https://doi.org/10.1016/J.GEE.2022.02.002
50. P.J. Hall, M. Mirzaeian, S.I. Fletcher, F.B. Sillars, A.J.R. Rennie, G.O. Shitta-Bey, G. Wilson, A. Cruden, R. Carter, Energy storage in electrochemical capacitors: designing functional materials to improve performance. Energy Environ. Sci. 3 (2010). https://doi.org/10.1039/c0ee00004c
51. J. Liu, J. Wang, C. Xu, H. Jiang, C. Li, L. Zhang, J. Lin, Z.X. Shen, Advanced energy storage devices: basic principles, analytical methods, and rational materials design. Adv. Sci. 5 (2018). https://doi.org/10.1002/advs.201700322

52. G. Zamiri, A.S.M.A. Haseeb, P. Jagadish, M. Khalid, I. Kong, S.G. Krishnan, Three-dimensional graphene-TiO2-SnO2Ternary nanocomposites for high-performance asymmetric supercapacitors. ACS Omega **7** (2022). https://doi.org/10.1021/acsomega.2c05343
53. K. Yousefipour, R. Sarraf-Mamoory, A. Yourdkhani, Supercapacitive properties of nickel molybdate/rGO hybrids prepared by the hydrothermal method. Surf. Interfaces **29**, 101638 (2022). https://doi.org/10.1016/J.SURFIN.2021.101638
54. P. Mars, in IEEE Technology Time Machine Symposium on Technologies Beyond 2020. A survey of supercapacitors, their applications, power design with supercapacitors, and future directions, vol 2011 (TTM, 2011). https://doi.org/10.1109/TTM.2011.6005184
55. P.I.N.G. ZHU, D.A.N. GAO, T.A.O. LI, Research on the aging of micro-supercapacitor under the condition of longtime storage. J. Energy Storage **40**, 102766 (2021). https://doi.org/10.1016/J.EST.2021.102766
56. V.O. Makarov, M. Trontelj, Sintering and electrical conductivity of doped WO3. J. Eur. Ceram. Soc., 16 (1996). https://doi.org/10.1016/0955-2219(95)00204-9
57. S. Buathet, K. Simalaotao, P. Reunchan, V. Vailikhit, P. Teesetsopon, D. Raknual, N. Kitisripanya, A. Tubtimtae, Electrochemical performance of Bi2Te3 heterostructure thin film and Cu7Te4 nanocrystals on undoped and In3+-doped WO3 films for energy storage applications. Electrochim. Acta, 341 (2020). https://doi.org/10.1016/j.electacta.2020.136049
58. A.S. Khan, F.U. Khan, A survey of wearable energy harvesting systems. Int. J. Energy Res., 46 (2022). https://doi.org/10.1002/er.7394
59. R. Ragavan, A. Pandurangan, Exploration on magnetic and electrochemical properties of nitrogen and phosphorus Co-doped ordered mesoporous carbon for supercapacitor applications. Microporous Mesoporous Mater. **338**, 111959 (2022). https://doi.org/10.1016/J.MICROMESO.2022.111959
60. M. Singh, A. Sahoo, K.L. Yadav, Y. Sharma, Role of magnetism present in the cobaltites (ACo2O4 A = Co, Mn, and Fe) on the charge storage mechanism in aqueous supercapacitor. Appl. Surf. Sci. **568**, 150966 (2021). https://doi.org/10.1016/J.APSUSC.2021.150966
61. L.M. Da Silva, R. Cesar, C.M.R. Moreira, J.H.M. Santos, L.G. De Souza, B.M. Pires, R. Vicentini, W. Nunes, H. Zanin, Reviewing the fundamentals of supercapacitors and the difficulties involving the analysis of the electrochemical findings obtained for porous electrode materials. Energy Storage Mater. **27**, 555–590 (2020). https://doi.org/10.1016/J.ENSM.2019.12.015
62. S. Karthikeyan, B. Narenthiran, A. Sivanantham, L.D. Bhatlu, T. Maridurai, Supercapacitor: evolution and review. Mater. Today Proc. **46**, 3984–3988 (2021). https://doi.org/10.1016/J.MATPR.2021.02.526
63. A.E.-S. Etman, A.M. Ibrahim, F.A.-Z.M. Darwish, K.F. Qasim, A 10 years-developmental study on conducting polymers composites for supercapacitors electrodes: a review for extensive data interpretation. J. Ind. Eng. Chem. (2023). https://doi.org/10.1016/j.jiec.2023.03.008
64. I. Melkiyur, Y. Rathinam, P.S. Kumar, A. Sankaiya, S. Pitchaiya, R. Ganesan, D. Velauthapillai, A comprehensive review on novel quaternary metal oxide and sulphide electrode materials for supercapacitor: Origin, fundamentals, present perspectives and future aspects. Renew. Sust. Energ. Rev. **173**, 113106 (2023). https://doi.org/10.1016/J.RSER.2022.113106
65. S.N. Kazi, in *Encyclopedia of Energy Storage*. Phase changing materials based super capacitors (2022). https://doi.org/10.1016/b978-0-12-819723-3.00104-9
66. T.F. Yi, J.J. Pan, T.T. Wei, Y. Li, G. Cao, NiCo2S4-based nanocomposites for energy storage in supercapacitors and batteries. Nano Today **33** (2020). https://doi.org/10.1016/j.nantod.2020.100894
67. Y. Liu, S.P. Jiang, Z. Shao, Intercalation pseudocapacitance in electrochemical energy storage: recent advances in fundamental understanding and materials development. Mater Today Adv **7** (2020). https://doi.org/10.1016/j.mtadv.2020.100072
68. S. Yao, X. Zheng, X. Zhang, H. Xiao, F. Qu, X. Wu, Facile synthesis of flexible WO3 nanofibers as supercapacitor electrodes. Mater. Lett. **186** (2017). https://doi.org/10.1016/j.matlet.2016.09.085
69. N. Choudhary, C. Li, J. Moore, N. Nagaiah, L. Zhai, Y. Jung, J. Thomas, Asymmetric supercapacitor electrodes and devices. Adv. Mater. **29** (2017). https://doi.org/10.1002/adma.201605336
70. S.B. Patil, R.P. Nikam, C.D. Lokhande, R.S. Patil, Chemisynthesized tungsten oxide (WO3) electrodes for high-performance asymmetric supercapacitor application: effect of deposition time. J. Mater. Sci. Mater. Electron. **34** (2023). https://doi.org/10.1007/s10854-023-11384-9
71. L. Zhang, X.S. Zhao, Carbon-based materials as supercapacitor electrodes. Chem. Soc. Rev. **38** (2009). https://doi.org/10.1039/b813846j
72. Y. Meng, J. Yin, L. Wang, X. Yang, X. Li, Y. Jiang, Facile WO3@PANI composite film for applications in doule-layer photoelectrochromic supercapacitors. Mater. Lett. **335** (2023). https://doi.org/10.1016/j.matlet.2022.133809
73. J. Cherusseri, D. Pandey, J. Thomas, Symmetric, asymmetric, and battery-type supercapacitors using two-dimensional nanomaterials and composites. Batter Supercaps **3** (2020). https://doi.org/10.1002/batt.201900230
74. P. Simon, Y. Gogotsi, Materials for electrochemical capacitors. Nat. Mater. **7** (2008). https://doi.org/10.1038/nmat2297
75. R. Velmurugan, P. Alagammai, M. Ulaganathan, B. Subramanian, High performance: In situ annealed partially pressurized pulsed laser deposited WO3& V2O5thin film electrodes for use as flexible all solid state supercapbatteries. J. Mater. Chem. A Mater. **8** (2020). https://doi.org/10.1039/d0ta07683j
76. K.K. Kar Editor, Springer series in materials science 302 Handbook of nanocomposite supercapacitor materials II performance, 2020. http://www.springer.com/series/856
77. S. Sharma, P. Chand, Supercapacitor and electrochemical techniques: a brief review. Results Chem. **5** (2023). https://doi.org/10.1016/j.rechem.2023.100885
78. M. Khot, A. Kiani, A review on the advances in electrochemical capacitive charge storage in transition metal oxide electrodes for pseudocapacitors. Int. J. Energy Res. **46** (2022). https://doi.org/10.1002/er.8763
79. P.A. Shinde, V.C. Lokhande, A.M. Patil, T. Ji, C.D. Lokhande, Single-step hydrothermal synthesis of WO3-MnO2 composite as an active material for all-solid-state flexible asymmetric supercapacitor. Int. J. Hydrog. Energy **43**, 2869–2880 (2018). https://doi.org/10.1016/J.IJHYDENE.2017.12.093
80. N. Meddings, M. Heinrich, F. Overney, J.S. Lee, V. Ruiz, E. Napolitano, S. Seitz, G. Hinds, R. Raccichini, M. Gaberšček, J. Park, Application of electrochemical impedance spectroscopy to commercial Li-ion cells: a review. J. Power Sources **480**, 228742 (2020). https://doi.org/10.1016/J.JPOWSOUR.2020.228742
81. S. Zhang, N. Pan, Supercapacitors performance evaluation. Adv. Energy Mater. **5** (2015). https://doi.org/10.1002/aenm.201401401
82. H. Feng, M. Zheng, H. Dong, Y. Xiao, H. Hu, Z. Sun, C. Long, Y. Cai, X. Zhao, H. Zhang, B. Lei, Y. Liu, Three-dimensional honeycomb-like hierarchically structured carbon for high-performance supercapacitors derived from high-ash-content sewage sludge. J. Mater. Chem. A Mater. **3** (2015). https://doi.org/10.1039/c5ta03217b
83. J. Xiao, Q. Li, Y. Bi, M. Cai, B. Dunn, T. Glossmann, J. Liu, T. Osaka, R. Sugiura, B. Wu, J. Yang, J.G. Zhang, M.S. Whittingham, Understanding and applying coulombic efficiency in

lithium metal batteries. Nat. Energy **5** (2020). https://doi.org/10.1038/s41560-020-0648-z
84. G. Gautham Prasad, N. Shetty, S. Thakur, K.B. Rakshitha, Bommegowda, supercapacitor technology and its applications: a review. IOP Conf Ser Mater Sci Eng (2019). https://doi.org/10.1088/1757-899X/561/1/012105
85. J. Matsuda, K. Yoshida, Y. Sasaki, N. Uchiyama, E. Akiba, In situ observation on hydrogenation of Mg-Ni films using environmental transmission electron microscope with aberration correction. Appl. Phys. Lett. **105** (2014). https://doi.org/10.1063/1.4894101
86. G. Mineo, E. Bruno, S. Mirabella, Advances in WO3-based supercapacitors: state-of-the-art research and future perspectives. Nanomaterials **13** (2023). https://doi.org/10.3390/nano13081418
87. F. Zheng, J. Wang, W. Liu, J. Zhou, H. Li, Y. Yu, P. Hu, W. Yan, Y. Liu, R. Li, Q. Zhen, J. Zhang, Novel diverse-structured h-WO3 nanoflake arrays as electrode materials for high performance supercapacitors. Electrochim. Acta **334** (2020). https://doi.org/10.1016/j.electacta.2020.135641
88. F. Shi, J. Li, J. Xiao, X. Zhao, H. Li, Q. An, S. Zhai, K. Wang, L. Wei, Y. Tong, Three-dimensional hierarchical porous lignin-derived carbon/WO3 for high-performance solid-state planar micro-supercapacitor. Int. J. Biol. Macromol. **190** (2021). https://doi.org/10.1016/j.ijbiomac.2021.08.183
89. Z. Shao, X. Fan, X. Liu, Z. Yang, L. Wang, Z. Chen, W. Zhang, Hierarchical micro/nanostructured WO3 with structural water for high-performance pseudocapacitors. J. Alloys Compd. **765**, 489–496 (2018). https://doi.org/10.1016/J.JALLCOM.2018.06.192
90. J. Jia, X. Liu, R. Mi, N. Liu, Z. Xiong, L. Yuan, C. Wang, G. Sheng, L. Cao, X. Zhou, X. Liu, Self-assembled pancake-like hexagonal tungsten oxide with ordered mesopores for supercapacitors. J. Mater. Chem. A Mater. **6** (2018). https://doi.org/10.1039/c8ta05292a
91. D. Zhou, F. Shi, D. Xie, D.H. Wang, X.H. Xia, X.L. Wang, C.D. Gu, J.P. Tu, Bi-functional Mo-doped WO3 nanowire array electrochromism-plus electrochemical energy storage. J. Colloid Interface Sci. **465**, 112–120 (2016). https://doi.org/10.1016/J.JCIS.2015.11.068
92. R. Wang, L. Feng, W. Yang, Y. Zhang, Y. Zhang, W. Bai, B. Liu, W. Zhang, Y. Chuan, Z. Zheng, H. Guan, Effect of different binders on the electrochemical performance of metal oxide anode for Lithium-Ion batteries. Nanoscale Res. Lett. **12** (2017). https://doi.org/10.1186/s11671-017-2348-6
93. A.V. Salkar, S.V. Bhosale, P.P. Morajkar, in *Advances in metal oxides and their composites for emerging applications*. Nanostructured WO3−x based advanced supercapacitors for sustainable energy applications (2022). https://doi.org/10.1016/B978-0-323-85705-5.00001-4
94. Y. Baek, K. Yong, Controlled growth and characterization of tungsten oxide nanowires using thermal evaporation of WO3 powder. J. Phys. Chem. C **111** (2007). https://doi.org/10.1021/jp0659857
95. Z. Hai, M. Karbalaei Akbari, Z. Wei, C. Xue, H. Xu, J. Hu, S. Zhuiykov, Nano-thickness dependence of supercapacitor performance of the ALD-fabricated two-dimensional WO3. Electrochim. Acta **246** (2017). https://doi.org/10.1016/j.electacta.2017.06.095
96. T.K. Shivasharma, N. Upadhyay, T.B. Deshmukh, B.R. Sankapal, Exploring vacuum-assisted thin films toward supercapacitor applications: present status and future prospects. ACS Omega **8**, 37685–37719 (2023). https://doi.org/10.1021/acsomega.3c05285
97. D. Evecan, E. Zayim, Highly uniform electrochromic tungsten oxide thin films deposited by e-beam evaporation for energy saving systems. Curr. Appl. Phys. **19** (2019). https://doi.org/10.1016/j.cap.2018.12.006
98. S. Yao, F. Qu, G. Wang, X. Wu, Facile hydrothermal synthesis of WO3 nanorods for photocatalysts and supercapacitors. J. Alloys Compd. **724**, 695–702 (2017). https://doi.org/10.1016/J.JALLCOM.2017.07.123
99. R. Hinterding, A. Feldhoff, Two-dimensional oxides: recent progress in nanosheets. Z. Phys. Chem. **233** (2018). https://doi.org/10.1515/zpch-2018-1125
100. S. Wang, H. Xu, T. Hao, M. Xu, J. Xue, J. Zhao, Y. Li, 3D conifer-like WO3 branched nanowire arrays electrode for boosting electrochromic-supercapacitor performance. Appl. Surf. Sci. **577** (2022). https://doi.org/10.1016/j.apsusc.2021.151889
101. T. Jin, D. Xu, P. Diao, W.P. He, H.W. Wang, S.Z. Liao, Tailored preparation of WO3 nano-grassblades on FTO substrate for photoelectrochemical water splitting. CrystEngComm **18** (2016). https://doi.org/10.1039/c6ce01186a
102. F. Mitsugi, E. Hiraiwa, T. Ikegami, K. Ebihara, R.K. Thareja, WO3 thin films prepared by pulsed laser deposition. Jpn. J. Appl. Phys. **41** (2002). https://doi.org/10.1143/jjap.41.5372
103. R. Velmurugan, M. Aishwarya, K. Balamurugan, K. Nivedha, B. Subramanian, Influencing In situ tuned nanostructures of pulsed laser ablated Co3O4 & WO3 thin film electrodes for binder free flexible operando hybrid supercapacitor devices. Electrochim. Acta **419** (2022). https://doi.org/10.1016/j.electacta.2022.140371
104. C. Gao, X. Guo, L. Nie, X. Wu, L. Peng, J. Chen, A review on WO3 gasochromic film: Mechanism, preparation and properties. Int. J. Hydrog. Energy **48** (2023). https://doi.org/10.1016/j.ijhydene.2022.10.100
105. M. Hepel, M.A. Petrukhina, V. Samuilov, High Power-Density WO3-x–Grafted Corannulene-Modified graphene nanostructures for Micro-Supercapacitors. J. Electroanal. Chem. **928**, 116990 (2023). https://doi.org/10.1016/J.JELECHEM.2022.116990
106. R. Dadashi, M. Bahram, M. Faraji, Polyaniline-tungsten oxide nanocomposite co-electrodeposited onto anodized graphene oxide nanosheets/graphite electrode for high performance supercapacitor device. J. Appl. Electrochem. **53** (2023). https://doi.org/10.1007/s10800-022-01812-9
107. M. Deepa, M. Kar, D.P. Singh, A.K. Srivastava, S. Ahmad, Influence of polyethylene glycol template on microstructure and electrochromic properties of tungsten oxide. Sol. Energy Mater. Sol. Cells **92** (2008). https://doi.org/10.1016/j.solmat.2007.01.024
108. Y. Li, W. Zhou, Z. Huang, Q. Pan, X. Zhao, M. Zhang, X. Hao, D. Li, J. Xu, Flexible Ce-doped WO3 nanowire arrays with enriched oxygen vacancies for soft-packaged asymmetric supercapacitor. Appl. Surf. Sci. **655** (2024). https://doi.org/10.1016/j.apsusc.2024.159616
109. T.H.Q. Nguyen, F. Eberheim, S. Göbel, P. Cop, M. Eckert, T.P. Schneider, L. Gümbel, B.M. Smarsly, D. Schlettwein, Enhancing the spectroelectrochemical performance of WO3 Films by use of structure-directing agents during Film growth. Appl. Sci. (Switzerland) **12** (2022). https://doi.org/10.3390/app12052327
110. K.W. Kim, T.Y. Yun, S.H. You, X. Tang, J. Lee, Y. Seo, Y.T. Kim, S.H. Kim, H.C. Moon, J.K. Kim, Extremely fast electrochromic supercapacitors based on mesoporous WO3 prepared by an evaporation-induced self-assembly. NPG Asia Mater. **12** (2020). https://doi.org/10.1038/s41427-020-00257-w
111. U.V. Shembade, S.D. Dhas, M.G. Magadum, S.R. Gurav, P.G. Raje, R.G. Sonkawade, S.B. Wategaonkar, S.R. Ghatage, M.A. Gaikwad, J.H. Kim, V.G. Parale, H.H. Park, A.V. Moholkar, Investigating the effect of electrolyte and its concentration dependence on WO3 nanosheet as an efficient electrode for supercapacitors: Effect of Redox Additive. J. Phys. Chem. Solids **183** (2023). https://doi.org/10.1016/j.jpcs.2023.111609
112. J. Gutpa, H. Shaik, K. Naveen Kumar, S.A. Sattar, PVD techniques proffering avenues for fabrication of porous tungsten

oxide (WO3) thin films: A review. Mater. Sci. Semicond. Process. **143** (2022). https://doi.org/10.1016/j.mssp.2022.106534
113. W. Sun, H. Liu, G. Xu, C. Li, J. Bai, J. Liu, Enhanced capacitive performance of WO3@W18O49-CNFs-based flexible electrode as a high performance supercapacitor. Ionics (Kiel) **26** (2020). https://doi.org/10.1007/s11581-019-03369-8
114. L.O. Animasahun, B.A. Taleatu, S.A. Adewinbi, R.A. Busari, E. Omotoso, O.E. Adewumi, A.Y. Fasasi, Rapid synthesis and characterizations of defect-enhanced WO3-δ thin film electrode for effective energy storage application in asymmetric supercapacitor devices. Mater. Res. Bull. **167** (2023). https://doi.org/10.1016/j.materresbull.2023.112378
115. S. Sengupta, M. Kundu, rGO-wrapped Hexagonal WO3 Nanorod as Advanced Electrode Material for Asymmetric Electrochemical Supercapacitors. Energy Technol. **11** (2023). https://doi.org/10.1002/ente.202300078
116. M. Karuppaiah, P. Sakthivel, S. Asaithambi, V. Balaji, G. Vijayaprasath, R. Yuvakkumar, G. Ravi, In-situ deposition of amorphous Tungsten(VI) oxide thin-film for solid-state symmetric supercapacitor. Ceram. Int. **48**, 2510–2521 (2022). https://doi.org/10.1016/J.CERAMINT.2021.10.033
117. V.V. Mohan, P.M. Anjana, R.B. Rakhi, One pot synthesis of tungsten oxide nanomaterial and application in the field of flexible symmetric supercapacitor energy storage device. Mater. Today Proc. **62** (2022). https://doi.org/10.1016/j.matpr.2022.04.046
118. M. Faraji, R. Khalilzadeh Soltanahmadi, H. Mohammadzadeh Aydisheh, B. Mostafavi Bavani, 2.0-V flexible all-solid-state symmetric supercapacitor device with high electrochemical performance composed of MWCNTs-WO3-graphite sheet. Ionics (Kiel) **26** (2020). https://doi.org/10.1007/s11581-020-03502-y
119. M. Ju, Y. Tian, Y. Luo, X. Bin, W. Que, Solvothermal synthesis of Ti3C2Tx/WO3−x flexible and self-standing films for aqueous proton supercapacitor electrodes. Mater. Lett. **297** (2021). https://doi.org/10.1016/j.matlet.2021.129901
120. R.S. Karmur, D. Gogoi, A. Biswas, C. Prathibha, M.R. Das, N.N. Ghosh, Nanocomposite having hierarchical architecture of MXene-WO3 nanorod@rGOsponge and porous carbon for cathode and anode materials for high-performance flexible all-solid-state asymmetric supercapacitor device. Appl. Surf. Sci. **623** (2023). https://doi.org/10.1016/j.apsusc.2023.157042
121. A.K. Das, S. Paria, A. Maitra, L. Halder, A. Bera, R. Bera, S.K. Si, A. De, S. Ojha, S. Bera, S.K. Karan, B.B. Khatua, Highly Rate Capable Nanoflower-like NiSe and WO3@PPy Composite Electrode Materials toward High Energy Density Flexible All-Solid-State Asymmetric Supercapacitor. ACS Appl. Electron. Mater. **1** (2019). https://doi.org/10.1021/acsaelm.9b00164
122. R. Barik, A.K. Yadav, S.N. Jha, D. Bhattacharyya, P.P. Ingole, Two-dimensional tungsten oxide/selenium nanocomposite fabricated for flexible supercapacitors with higher operational voltage and their charge storage mechanism. ACS Appl. Mater. Interfaces **13** (2021). https://doi.org/10.1021/acsami.0c15818
123. S.H. Ji, N.R. Chodankar, W.S. Jang, D.H. Kim, High mass loading of h-WO3 and α-MnO2 on flexible carbon cloth for high-energy aqueous asymmetric supercapacitor. Electrochim. Acta **299**, 245–252 (2019). https://doi.org/10.1016/J.ELECTACTA.2018.12.187
124. Z. Pan, C. Yang, Z. Chen, X. Ji, Construction of Ti3C2Tx/WOx heterostructures on carbon cloth for ultrahigh-mass loading flexible supercapacitor. Nano Res. **15** (2022). https://doi.org/10.1007/s12274-022-4561-6
125. X. Lu, T. Zhai, X. Zhang, Y. Shen, L. Yuan, B. Hu, L. Gong, J. Chen, Y. Gao, J. Zhou, Y. Tong, Z.L. Wang, WO 3-x@Au@MnO 2 core-shell nanowires on carbon fabric for high-performance flexible supercapacitors. Adv. Mater. **24**, 938–944 (2012). https://doi.org/10.1002/adma.201104113
126. Z. Bi, X. Li, Y. Chen, X. Xu, S. Zhang, Q. Zhu, Bi-functional flexible electrodes based on tungsten trioxide/zinc oxide nanocomposites for electrochromic and energy storage applications. Electrochim. Acta **227** (2017). https://doi.org/10.1016/j.electacta.2017.01.003
127. R. Huang, J. Zhang, Z. Dong, H. Lin, S. Han, Oxygen Vacancy Engineering of TiO2/WO3 Composites on a Carbon Fiber as Advanced Electrodes for High-Performance Flexible Supercapacitors. ACS Appl. Energy Mater. **6** (2023). https://doi.org/10.1021/acsaem.2c03553
128. P.O. Anikpa, A.U. Mee, A.C. Nwanya, A.C. Nkele, D.B. Malavekar, R.U. Osuji, N. Nwulu, C.D. Lokhande, F.I. Ezema, Asymmetric supercapacitor performance of hydrothermally-synthesized MWCNT-WO3 composite electrode. J. Energy Storage **81** (2024). https://doi.org/10.1016/j.est.2024.110439
129. L. Dong, C. Xu, Y. Li, Z.H. Huang, F. Kang, Q.H. Yang, X. Zhao, Flexible electrodes and supercapacitors for wearable energy storage: A review by category. J. Mater. Chem. A Mater. **4** (2016). https://doi.org/10.1039/c5ta10582j
130. P.E. Lokhande, U.S. Chavan, S. Bhosale, A. Kalam, S. Deokar, in *Flexible Supercapacitor Nanoarchitectonics*. New-Generation Materials for Flexible Supercapacitors (2021). https://doi.org/10.1002/9781119711469.ch11
131. P. Dutta, S.C. Karumuthil, R. Roy, A.K. Singh, Highly Stable Poly(o-methoxyaniline)/WO3-Nanoflower Composite-Based Electrochromic Supercapacitors with Real-Time Charge Indication. ACS Appl. Polym. Mater. **5** (2023). https://doi.org/10.1021/acsapm.3c00311
132. E. Muslu, E. Eren, A. Uygun Oksuz, Evaluation of Supercapacitor Properties of Radio Frequency Sputter Binder-Free and Nanosandwich WO3/SiO2/WO3 Thin Film. Energy Technol. (2023). https://doi.org/10.1002/ente.202300574
133. D. Majumdar, in *Flexible Supercapacitor Nanoarchitectonics*. Aqueous Electrolytes for Flexible Supercapacitors (2021). https://doi.org/10.1002/9781119711469.ch13
134. Y.R. Beg, G.R. Nishad, P. Singh, in *Flexible Supercapacitor Nanoarchitectonics*. Organic Electrolytes for Flexible Supercapacitors (2021). https://doi.org/10.1002/9781119711469.ch6
135. S. Shahzad, A. Shah, E. Kowsari, F.J. Iftikhar, A. Nawab, B. Piro, M.S. Akhter, U.A. Rana, Y. Zou, Ionic Liquids as Environmentally Benign Electrolytes for High-Performance Supercapacitors. Global Chall. **3** (2019). https://doi.org/10.1002/gch2.201800023
136. H. Dai, G. Zhang, D. Rawach, C. Fu, C. Wang, X. Liu, M. Dubois, C. Lai, S. Sun, Polymer gel electrolytes for flexible supercapacitors: Recent progress, challenges, and perspectives. Energy Storage Mater. **34** (2021). https://doi.org/10.1016/j.ensm.2020.09.018
137. I.K. Durga, D.K. Kulurumotlakatla, T. Ramachandran, Y.A. Kumar, D.A. Reddy, K.V.G. Raghavendra, A.A. Alothman, S.S. Rao, Synergy unleashed: NiMoO4/WO3/NF nanoflowers elevate for supercapacitor performance. J. Phys. Chem. Solids **186** (2024). https://doi.org/10.1016/j.jpcs.2023.111811
138. V. Castiglia, N. Campagna, C. Spataro, C. Nevoloso, F. Viola, R. Miceli, Modelling, simulation and characterization of a supercapacitor, in: 20th IEEE Mediterranean Electrotechnical Conference, MELECON 2020 - Proceedings, 2020. https://doi.org/10.1109/MELECON48756.2020.9140474.
139. V. Castiglia, N. Campagna, A.O.D.I. Tommaso, R. Miceli, C. Nevoloso, F. Pellitteri, C. Puccio, F. Viola, Modeling, Simulation, and Characterization of a Supercapacitor in Automotive Applications. IEEE Trans. Ind. Appl. **58** (2022). https://doi.org/10.1109/TIA.2022.3142707